CHAPTER ONE

INTRODUCTION

1.1 Background

The electricity supply industry is undergoing a profound transformation worldwide. Market forces, scarcer natural resources, and an ever increasing demand for electricity are some of the drivers responsible for such an unprecedented change. Against this background of rapid evolution, the expansion programs of many utilities are being thwarted by a variety of well-founded, environmental, land-use, and regulatory pressures that prevent the licensing and building of new transmission lines and electricity generating plants. An in-depth analysis of the options available for maximizing existing transmission assets, with high levels of reliability and stability, has pointed in the direction of power electronics [1].

An electrical power system can be seen as the interconnection of generating sources and customer loads through a network of transmission lines, transformers, and ancillary equipment. Based on their structure, power systems can be broadly classified into meshed and longitudinal systems. Meshed systems can be found in regions with a high population density and where it is possible to build power stations close to load demand centers. Longitudinal systems are found in regions where large amounts of power have to be transmitted over long distances from power stations to load demand centers [2].

The large interconnected transmission networks (made up of predominantly overhead transmission lines) are susceptible to faults caused by lightning discharges and decrease in insulation clearances by undergrowth, while the loads in a power system vary by the time of the day in general, they are also subject to variations

caused by the weather (ambient temperature) and other unpredictable factors. The generation pattern in a deregulated environment also tends to be variable (and hence less predictable). Thus, the power flow in a transmission line can vary even under normal, steady state conditions. The occurrence of a contingency (due to the tripping of a line, generator) can result in a sudden increase/decrease in the power flow. This can result in overloading of some lines and consequent threat to system security [2-3].

The increase in the loading of the transmission lines sometimes can lead to collapse in the network due to the shortage of reactive power delivered at the load centers. This is due to the increased consumption of the reactive power in the transmission network and the characteristics of the load (such as induction motors supplying constant torque) [2]. Examples of operating problems to which unregulated active and reactive power flows may give rise are:

- loss of system stability,
- power flow loops,
- high transmission losses,
- voltage limit violations,
- an inability to utilize transmission line capability up to the thermal limit,
- and cascade tripping in the long term,

The required safe operating margin can be substantially reduced by the introduction of fast dynamic control over reactive and active power by high power electronic controllers. A new technological thinking that comes under the generic title of FACTS – an acronym for flexible alternating current transmission systems. This can make the AC transmission network "flexible" to adapt to the changing conditions caused by contingencies and load variations [2].

1.2 Inherent Limitations of Transmission Systems

The characteristics of a given power system evolve with time, as load grows and generation is added. If the transmission facilities are not upgraded sufficiently the power system becomes vulnerable to steady-state and transient stability problems, as stability margins become narrower.

The ability of the transmission system to transmit power becomes impaired by one or more of the following steady-state and dynamic limitations:

- angular stability;
- voltage magnitude;
- thermal limits;
- transient stability;
- Dynamic stability.

These limits define the maximum electrical power to be transmitted without causing damage to transmission lines and electric equipment. In principle, limitations on power transfer can always be relieved by the addition of new transmission and generation facilities. Alternatively, FACTS controllers can enable the same objectives to be met with no major alterations to system layout. The potential benefits brought about by FACTS controllers include reduction of operation and transmission investment cost, increased system security and reliability, increased power transfer capabilities, and an overall enhancement of the quality of the electric energy delivered to customers [2].

1.3 Problem Statement

Power systems operation becomes more stressed as the load demand increases all over the world. This rapid increase in load demand forces power systems to operate near critical limits due to economic and environmental constraints. In economic constrain aspect, investment costs of generation and transmission systems play great in power market in order to be competitive in power market therefore, systems will operate at critical limits since investment costs are high and all this will make construction of new power plants and transmission lines and operation of existing ones should be carried out efficiently[4].

Environmental constraints have negative effect on construction of new power plants and transmission lines. Great portion of the energy produced is consumed by big cities. Most of the time, it is impossible to build generation units near crowded cities which causes significant loss of energy due to long transmission lines [4].

Since generation and transmission units have to be operated at critical limits voltage stability problems may occur in power system when change in load occur demand or fault "there is an increase in load demand". Voltage instability is one of the main problems in power systems. In voltage stability problem some or all buses voltages decrease due to insufficient power delivered to loads [4].

1.4 Dissertation Objectives

Sudan electric power system is undergoing change as result of constant power demand increase, thus it operates beyond its stability and thermal limit. This drastically affects the power quality delivered. Transmission systems should be flexible to respond to generation and load patterns. The focus of this dissertation is to study how different FACTS controllers Static Var Compensator (SVC) and

Thyristor Control Series Compensator (TCSC) reduce real power losses and improving voltage profile in the Sudan national Grid.

1.5 Methodology / approach:

- Study and analyze the Sudan national electrical grid.
- Select the optimal location and sizing of SVC and TCSC achieved using stability indices at different power loading.
- Incorporate TCSC and SVC with the grid according to indices of stability.
- Analyzing the obtained results.
- NEPLAN software and Matpower Tools are used to implement this study and obtain the results.

1.6 Thesis Layout

This dissertation consists of five chapters. Chapter two gives brief description for various FACTS controllers, and then represents a full discussion on SVC and TCSC, their model, control capabilities and operating principles. The placement strategy of SVC & TCSC controllers at the optimal locations in Sudanese electrical network is described in chapter three. In chapter four the approach developed is implemented on real case Sudanese national grid. Improvement of voltage profile and power loss reduction is also investigated. Finally conclusions and scope of future work are given in chapter five.

CHAPTER TWO

LITERATURE REVIEW

2.1 Introduction

Flexible AC Transmission System (FACTS) is defined as 'a power electronic based system and other static equipment that provide control of one or more AC transmission system parameters [2, 3]. Also defined as 'Alternating current transmission systems incorporating power electronic-based and other static controllers to enhance controllability and increase power transfer capability' [5]. There are two main objectives of FACTS controllers which are increasing the power transfer capability of transmission system and limit power flow over designated lines. In current power market, control of active and reactive power flow in a transmission line becomes a necessity aspect. Entry of more power generation companies has increased the need for enhanced secured operation of power systems, which are facing the threat of voltage instability leading to voltage collapse and also for minimization of active power loss leading to reduction in electricity cost. This achieved by load compensation which consists of improvement in power factor, balancing of real power drawn from the supply, better voltage regulation of large fluctuating loads, and also achieved by voltage support at a given terminal of the transmission line [6,7].

2.2 Reactive Power Controller

Power flow control has traditionally relied on generator control, voltage regulation by means of tap-changing and phase-shifting transformers, and reactive power plant compensation switching. Phase-shifting transformers have been used for the purpose of regulating active power in alternating current (AC) transmission networks [2].

Series reactors are used to reduce power flow and short-circuit levels at designated locations of the network. Conversely, series capacitors are used to shorten the electrical length of lines, hence increasing the power flow. In general, series compensation is switched on and off according to load and voltage conditions. For instance, in longitudinal power systems, series capacitive compensation is bypassed during minimum loading in order to avoid transmission line overvoltage due to excessive capacitive effects in the system. Conversely, series capacitive compensation is fully utilized during maximum loading, aiming at increasing the transfer of power without subjecting transmission lines to overloads [2].

2.3 Compensator classification with regard to their connection in the network.

The compensator in terms of connection can be classified as:

- 1. Series controllers,
- 2. Shunt Compensator.
- 3. Combined series-series Compensator.
- 4. Combined shunt-series Compensator.

2.3.1 Series Compensator:

Series controllers, in FACTS technology, are used to inject voltage in series with the line. In simplest form, a variable impedance multiplied by the current flow through it represents an injected series voltage in the line. If the series voltage in phase quadrature with the line current, the series controller only supplied or absorbs

variable reactive power. Real power is involved for any other phase relationship between the injected voltage and the line current. The symbolic representation of series FACTS controller is shown in Figure 2.1 [8].

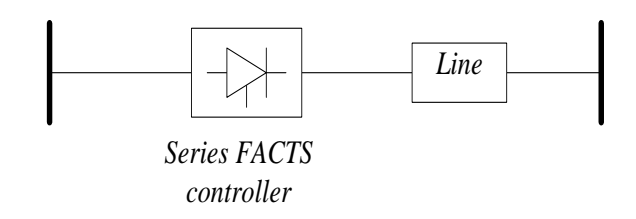


Figure 2.1: The symbolic of series compensation.

It controls the effective line parameters by connecting a variable reactance in series with the line. This increase the transmission line capability which in turn reduces transmission line net impedance. Example of Series compensator are Static Synchronous Series Compensator (SSSC) and Thyristor Control Series Compensator (TCSC) [7].

2.3.2 Shunt Compensator:

Similar to series controller, *shunt Compensator* have variable impedance or variable source or combination of both as shown in Figure 2.2. All shunt connected FACTS controllers inject current into the bus at the point of connection. The shunt impedance may be variable to vary the injected current. As long as this injected current is in phase quadrature with the line voltage, the shunt controller only supplies or absorbs variable reactive power. Any other phase relationship of the generated current with line voltage will involve real power flow [8].

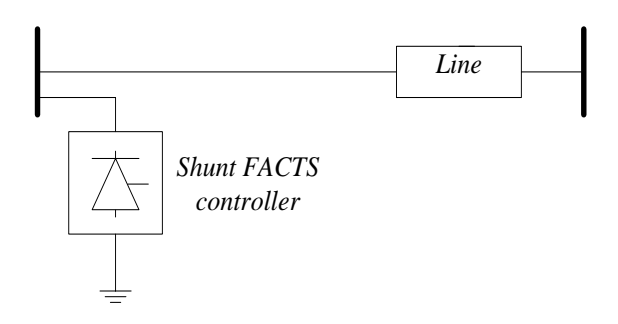


Figure 2.2: The symbolic of shunt compensation.

The operational pattern is same with an ideal synchronous machine that generates balanced three phase voltages with controllable amplitude and phase angle. The characteristics enables shunt compensators to be represented in positive sequence power flow studies with zero active power generation and reactive limits. Examples are Static Synchronous Compensator (STATCOM), Static Var Compensator (SVC) [7].

2.3.3 Series-Series Compensator:

It is the combination of two or more static synchronous compensators coupled through a common dc link to enhance bi-directional flow of real power between the ac terminals of SSSC and are controlled to provide independent reactance compensation for the adjustment of real power flow in each line and maintain the desired of reactive power flow among the power lines. Example of series – series compensator is Interline Power Flow Controller (IPFC) [7]. Figure 2.3 represent the symbolic of series- series compensation.

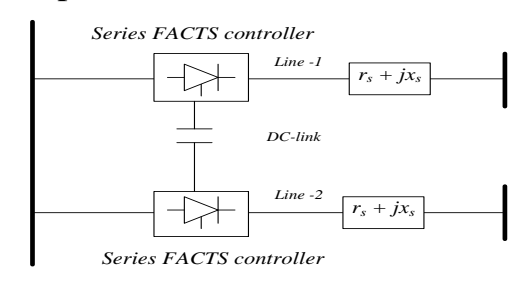


Figure 2.3: The symbolic of series- series compensation.

2.3.4 Series-Shunt Compensator:

It allows the simultaneous control of active power flow, reactive power flow and voltage magnitude at the series shunt compensator terminals. The active power control takes place between the series converter and the AC system, while the shunt converter generates or absorbs reactive power so as to provide voltage magnitude at the point of connection of the device and the AC system. Example of the series-shunt compensator is the unified power flow controller (UPFC) and thyristor controlled phase shifting Transformer (TCPST) [7]. Figure 2.4 represent the symbolic of series-shunt compensation.

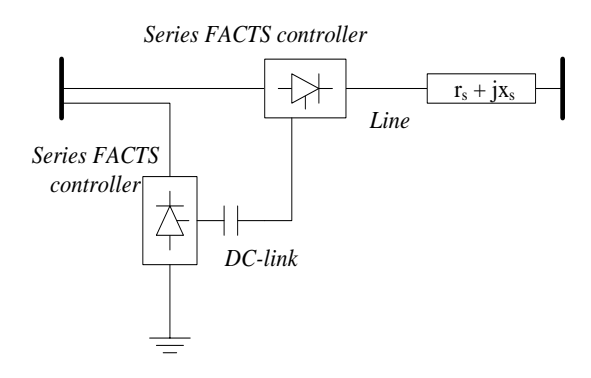


Figure 2.4: The symbolic of series- shunt compensation.

2.4 Classification of FACTS Controllers Based on Power Electronic Devices:

Depending on the power electronic devices used in the control, the FACTS controllers can be classified as

2.4.1 Variable impedance

2.4.1.1 Static VAR Compensator (SVC):

The SVC consists of a TCR in parallel with a bank of capacitors. From an operational point of view, the SVC behaves like a shunt-connected variable

reactance, which either generates or absorbs reactive power in order to regulate the voltage magnitude at the point of connection to the AC network. It is used extensively to provide fast reactive power and voltage regulation support. The firing angle control of the thyristor enables the SVC to have almost instantaneous speed of response. Generally they are two configurations of the SVC [2].

I. Shunt Variable susceptance model

The SVC consists of a group of shunt-connected capacitors and reactors banks with fast control action by means of thyristor switching circuits. From the operational point of view, the SVC can be considered as a variable shunt reactance that adjusts automatically according to the system operative conditions. Depending on the nature of the equivalent SVC's reactance, i.e., capacitive or inductive, the SVC draws either capacitive or inductive current from the network. Suitable control of this equivalent reactance allows voltage magnitude regulation at the SVC point of connection. The most popular configuration for continuously controlled SVC is the combination of either fix capacitor and thyristor controlled reactor or thyristor switched capacitor and thyristor controlled reactor. For steady-state analysis, both configurations can be modeled along similar lines [9]. A changing susceptance B_{svc} represents the fundamental frequency equivalent susceptance of all shunt modules making up the SVC as shown in Figure 2.5. is used to derive the SVC nonlinear power equations and the linearized equations required by Newton's method. With reference to Figure 2.5,

Bsvc

Figure 2.5: SVC susceptance model.

The current drawn by the SVC is

$$I_{SVC} = j B_{SVC} V_k$$
.....(2.1)

And the reactive power drawn by the SVC, which is also the reactive power injected at bus k, is

$$Q_{SVC} = Q_k = -V_k^2 B_{SVC}.$$
 (2.2)

The linearized equation is given by equation (2.3), where the equivalent susceptance B_{SVC} is taken to be the state variable:

$$\begin{bmatrix} \Delta P_k \\ \Delta Q_k \end{bmatrix}^{(i)} = \begin{bmatrix} 0 & 0 \\ 0 & Q_k \end{bmatrix}^{(i)} \begin{bmatrix} \Delta \theta_k \\ \Delta B_{svc}/B_{svc} \end{bmatrix}^{(i)} \dots (2.3)$$

At the end of iteration (i), the variable shunt susceptance B_{SVC} is updated according to:

$$B_{svc}^{(i)} = B_{svc}^{(i-1)} + \left(\frac{\Delta B_{svc}}{B_{svc}}\right)^{(i)} Bsvc^{(i-1)} \dots (2.4)$$

Where, V_K =voltage at bus k

 B_{svc} = Susceptance

 Q_{SVC} = reactive power drawn by SVC.

I_{SVC}= the current drawn by the SVC.

 Q_k = reactive power at bus k.

 P_k = active power at bus k.

The changing susceptance represents the total SVC susceptance necessary to maintain the nodal voltage magnitude at the specified value.

Once the level of compensation has been computed then the thyristor firing angle can be calculated. However, the additional calculation requires an iterative solution because the SVC susceptance and thyristor firing angle are nonlinearly related [2].

II. Firing angle model.

The equivalent reactance X_{SVC} , which is function of a changing firing angle α , is made up of the parallel combination of a thyristor controlled reactor (TCR) equivalent admittance and a fixed capacitive reactance as shown in Figure 2.6. This model provides information on the SVC firing angle required to achieve a given level of compensation [10].

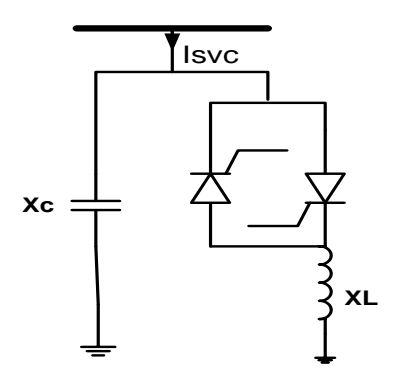


Figure 2.6: SVC firing angle model.

$$I_{svc} = j B_{svc} V_k$$

The fundamental frequency TCR equivalent reactance X_{TCR}

$$X_{TCR} = \frac{\pi X_L}{\sigma - \sin \sigma}.$$
 (2.5)

Where

$$\sigma = 2(\pi - \alpha), X_L = wL$$

And in terms of firing angle

$$X_{TCR} = \frac{\pi X_L}{2(\pi - \alpha) + \sin(2\alpha)}.$$
 (2.6)

 σ and α are conduction and firing angles respectively. At α =90, TCR conducts fully and the equivalent reactance X_{TCR} becomes X_L , while at α =180, TCR is blocked and its equivalent reactance becomes infinite. The SVC effective reactance X_{SVC} is determined by the parallel combination of X_C and X_{TCR}

$$X_{SVC} = \frac{\pi X_C X_L}{X_C [X_C [2((\pi - \alpha) + \sin 2\alpha] - \pi X_L]}.$$
(2.7)

Where $X_c=1/\omega C$

$$Q_K = -V_k^2 \left\{ \frac{X_C[X_C[2((\pi-\alpha) + \sin 2\alpha] - \pi X_L)]}{\pi X_C X_L} \right\}.$$
 (2.8)

The proposed model takes firing angle as the state variable in power flow formulation. From equation (2.8) the SVC linearized power flow equation can be written as

$$\begin{bmatrix} \Delta P_k \\ \Delta Q_k \end{bmatrix}^{(i)} = \begin{bmatrix} 0 & 0 \\ 0 & \frac{2V_k^2}{\pi X_L} [\cos(2\alpha) - 1] \end{bmatrix}^{(i)} \begin{bmatrix} \Delta \theta_k \\ \Delta \alpha \end{bmatrix}^{(i)} \dots (2.9)$$

At the end of iteration i, the variable firing angle α is updated according to

$$\alpha^{(i)} = \alpha^{(i-1)} + \Delta \alpha^{(i)}$$
.....(2.10)

$$V_k = V_{ref} + X_{SL} \cdot I_{SVC}$$
 (2.11)

Where V_k and I_{SVC} stand for controlling bus voltage and SVC current [11].

III. SVC V-I Characteristic

The typical steady-state control law of a SVC used here is depicted in Figure 2.7, and may be represented by the following voltage-current characteristic:

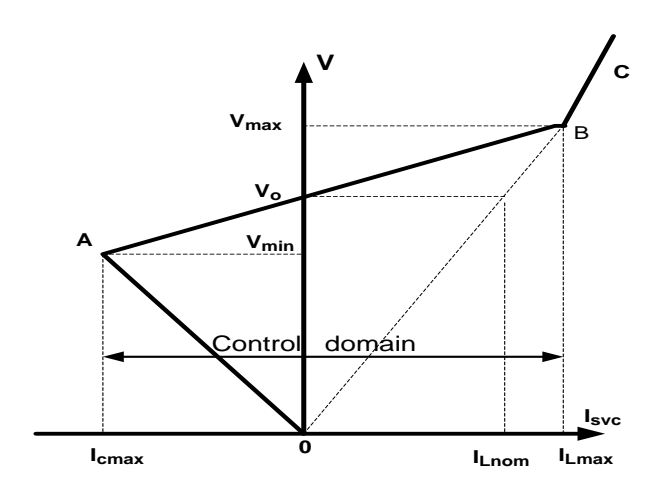


Figure 2.7: The V-I Characteristic Curve of SVC

• The linear control domain, in which the voltage control system is provided with appropriate reactive power resources, and the set-point can be defined any where on the AB characteristic. This domain is bounded by the reactive power Q_{Cmax} , supplied by the capacitors, and by the reactive power Q_{Lmax} absorbed by the reactor, that is $Q_{Cmax} \le Q \le Q_{Lmax}$.

In practice, a SVC uses droop control of the voltage at the regulated bus, with a slope of about 5%. The droop control means that the voltage at the regulated bus is controlled within a certain interval [V_{min} , V_{max}], instead of a constant voltage value V_{ref} .

- The high voltages domain (BC), resulted from the limitation in the inductive reactive power, i.e. $Q > Q_{Lmax}$. The SVC, in this case is out of the control area and it behaves like a fixed inductive susceptance.
- The low voltages domain (OA), resulted from the limitation in the capacitive reactive power, i.e. $Q < Q_{Cmax}$. The SVC, in this case is out of the control area and it behaves like a fixed capacitive susceptance [11].

The reason for including the SVC voltage current slope in power flow studies is compelling. The slope can be represented by connecting the SVC models to an auxiliary bus coupled to the high voltage bus by an inductive reactance consisting of the transformer reactance and the SVC slope, in per unit (p.u) on the SVC base. A simpler representation assumes that the SVC slope, accounting for voltage regulation is zero. This assumption may be acceptable as long as the SVC is operating within the limits, but may lead to gross errors if the SVC is operating close to its reactive limits [12-14].

2.4.1.2 Thyristor Controlled Series Compensator (TCSC),

It is designed based on TCR technology that has the ability to control the line impedance with a thyristor-controlled capacitor placed in series with the transmission line. It is used to increase the transmission line capability by installing a series capacitor that reduces the net series impedance thus allowing additional power to be transferred [15].

TCSC is a series compensation component which consists of a series capacitor bank shunted by thyristor controlled reactor Figure 2.8 shows the main circuit of a TCSC. The basic idea behind power flow control with the TCSC is to decrease or increase the overall lines effective series transmission impedance, by adding a capacitive or inductive reactive correspondingly. Thyristor Controlled Series Capacitor (TCSC) is one of the most effective FACTS controllers which offer smooth and flexible control of the line impedance with much faster response compared to the traditional control devices. TCSC can also enhance the stability, improve the dynamic characteristics of power system, and increase the transfer capability of the transmission system by reducing the transfer reactance between the buses at which the line is connected. However, to achieve the above mentioned benefits, the TCSC should be properly installed in the network with appropriate parameter settings.

For this reason, some performance indices must be satisfied, following factors can be considered in the optimal installation of TCSC, the topology of the system, the stability margin improvement, the power transmission capacity increasing, and the power blackout prevention [16].

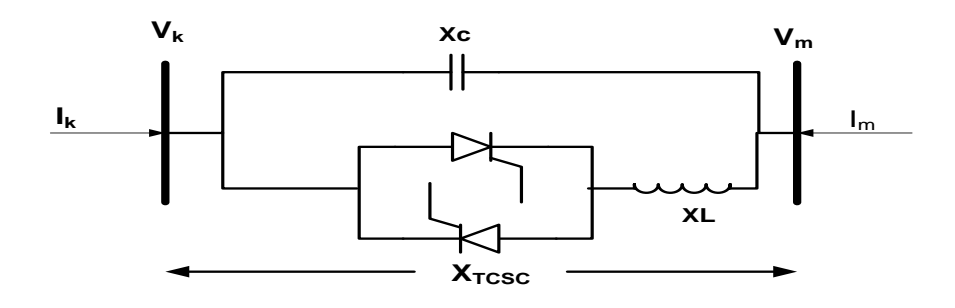


Figure 2.8: TCSC module

The firing angles of the thyristors are controlled to adjust the TCSC reactance according to the system control algorithm, normally in response to some system parameter variations. According to the variation of the thyristor firing angle or conduction angle, this process can be modeled as a fast switch between corresponding reactance offered to the power system. Assuming that the total current passing through the TCSC is sinusoidal, the equivalent reactance at the fundamental frequency can be represented as a variable reactance X_{TCSC} . The TCSC can be controlled to work either in the capacitive or the inductive zones avoiding steady state resonance. There is a steady-state relationship exist between the firing angle α and the reactance X_{TCSC} . This relationship can be described by the following equation:

$$X_{TCSC} = -Xc + C1 \left\{ 2(\pi - \alpha) + \sin \left[2(\pi - \alpha) \right] \right\} + C2 \cos^2(\pi - \alpha) \left\{ \overline{\omega} \tan \left[\overline{\omega} \left((\pi - \alpha) \right] - \tan(\pi - \alpha) \right\} \right\}.$$
(2.12)

Where

$$\overline{\omega} = \sqrt{\frac{X_C}{X_L}} \qquad \text{XLC} = \frac{X_C X_L}{X_C - X_L}$$

$$\text{C1} = \frac{X_C + X_{LC}}{X_C - X_L} \qquad \text{C2} = \frac{-X_{LC}^2}{\pi X_L}$$

For the purpose of power flow studies, the TCSC may be adequately represented by the equivalent reactance in Equation (2.12), which enables a straightforward representation of the TCSC in the form of a nodal transfer admittance matrix. This is derived with reference to the equivalent circuit in Figure 2.8, where it is assumed that the TCSC is connected between buses k and m.

The transfer admittance matrix relates the nodal currents injections, I_k and I_m , to the nodal voltages, V_k and V_m , via the variable TCSC reactance shown in the equivalent circuit of Figure 2.8.

2.4.1.2.1 Variable Series Impedance Power Flow Model

The TCSC power flow model presented in this section is based on the simple concept of a variable series reactance, the value of which is adjusted automatically to constrain the power flow across the branch to a specified value. The amount of reactance is determined efficiently using Newton's method. The changing reactance X_{TCSC} , shown in Figures 2.9(a) and 2.9(b), represents the equivalent reactance of all the series-connected modules making up the TCSC, when operating in either the inductive or the capacitive regions [2].

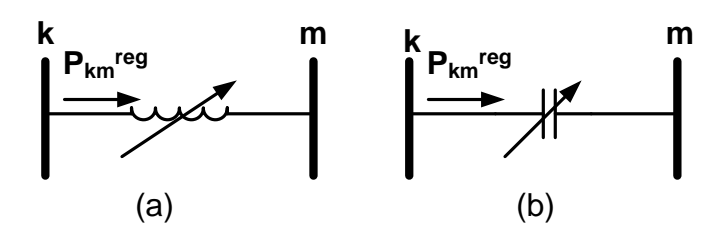


Figure 2.9: Thyristor-controlled series compensator equivalent circuit: (a) inductive and (b) capacitive operative regions

The transfer admittance matrix of the variable series compensator shown in Figure 2.9 is given by

$$\begin{bmatrix} I_K \\ I_m \end{bmatrix} = \begin{bmatrix} -jB_{kk} & jB_{km} \\ jB_{mk} & -jB_{mm} \end{bmatrix} \begin{bmatrix} V_k \\ V_m \end{bmatrix} \dots (2.13)$$

For inductive operation, we have

$$B_{kk} = B_{mm} = -\frac{1}{jX_{TCSC}}$$

$$B_{km} = B_{km} = \frac{1}{jX_{TCSC}}$$

And for capacitive operation the signs are reversed.

The active and reactive power equations at bus k are:

$$P_k = V_k V_m B_{km} \sin(\theta_k - \theta_m)....(2.14)$$

$$Q_k = -V_k^2 B_{kk} - V_k V_m B_{km} \cos(\theta_k - \theta_m) \dots (2.15)$$

In Newton–Raphson solutions these equations are linearized with respect to the series reactance. For the condition shown in Figure 2.9, where the series reactance regulates the amount of active power flowing from bus k to bus m at a value $P_{\rm km}^{\rm reg}$, the set of linearized power flow equations is:

$$\begin{bmatrix} \Delta P_{k} \\ \Delta P_{m} \\ \Delta Q_{k} \\ \Delta Q_{m} \\ \Delta P_{km} \end{bmatrix} = \begin{bmatrix} \frac{\partial P_{k}}{\partial \theta_{k}} & \frac{\partial P_{k}}{\partial \theta_{m}} & \frac{\partial P_{k}}{\partial V_{k}} V_{k} & \frac{\partial P_{k}}{\partial V_{m}} & \frac{\partial P_{k}}{\partial X_{TCSC}} X_{TCSC} \\ \frac{\partial P_{m}}{\partial \theta_{k}} & \frac{\partial P_{m}}{\partial \theta_{m}} & \frac{\partial P_{m}}{\partial V_{k}} V_{k} & \frac{\partial P_{m}}{\partial V_{m}} & \frac{\partial P_{m}}{\partial X_{TCSC}} X_{TCSC} \\ \frac{\partial Q_{k}}{\partial \theta_{k}} & \frac{\partial Q_{k}}{\partial \theta_{m}} & \frac{\partial Q_{k}}{\partial V_{k}} V_{k} & \frac{\partial Q_{k}}{\partial V_{m}} & \frac{\partial Q_{k}}{\partial X_{TCSC}} X_{TCSC} \\ \frac{\partial Q_{m}}{\partial \theta_{k}} & \frac{\partial Q_{m}}{\partial \theta_{m}} & \frac{\partial Q_{m}}{\partial V_{k}} V_{k} & \frac{\partial Q_{m}}{\partial V_{m}} V_{m} & \frac{\partial Q_{m}}{\partial X_{TCSC}} X_{TCSC} \\ \frac{\partial P_{km}^{X_{TCSC}}}{\partial \theta_{k}} & \frac{\partial P_{km}^{X_{TCSC}}}{\partial \theta_{m}} & \frac{\partial P_{km}^{X_{TCSC}}}{\partial V_{k}} V_{k} & \frac{\partial P_{km}^{X_{TCSC}}}{\partial V_{m}} V_{m} & \frac{\partial P_{km}^{X_{TCSC}}}{\partial X_{TCSC}} X_{TCSC} \end{bmatrix} \begin{bmatrix} \Delta \theta_{k} \\ \Delta \theta_{m} \\ \frac{\Delta V_{k}}{V_{k}} \\ \frac{\Delta V_{m}}{V_{m}} \\ \frac{\Delta X_{TCSC}}{X_{TCSC}} \end{bmatrix} \dots (2.16)$$

Where:

$$\Delta P_{km}^{X_{TCSC}} = P_{km}^{reg} - P_{km}^{X_{TCSC},cal}.$$
(2.17)

 $\Delta P_{km}^{X_{TCSC}}$ is the incremental change in series reactance; and $P_{km}^{X_{TCSC},cal}$ is the calculated power.

The state variable X_{TCSC} of the series controller is updated at the end of each iterative step according to [2]

$$X_{TCSC}^{(i)} = X_{TCSC}^{(i-1)} - \left(\frac{\Delta X_{TCSC}}{X_{TCSC}}\right)^{(i)} X_{TCSC}^{(i-1)}(2.18)$$

The TCSC is modeled as variable impedance, where the equivalent reactance of line X_{ij} is defined as:

$$X_{ij} = X_{line} + X_{TCSC}.$$
 (2.19)

Where, X_{line} is the transmission line reactance, and X_{TCSC} is the TCSC reactance. The level of the applied compensation of the TCSC usually varies between 20% inductive and 80% capacitive [17].

2.4.2 Variable Source Converter (VSC)

2.4.2.1 Static Synchronous Series Compensator (SSSC)

Static Synchronous Series Compensator is based on solid-state voltage source converter designed to generate the desired voltage magnitude independent of line current. SSSC consists of a converter, DC bus (storage unit) and coupling transformer. The dc bus uses the inverter to synthesize an ac voltage waveform that is inserted in series with transmission line through the transformer with an appropriate phase angle and line current. If the injected voltage is in phase with the line current it exchanges a real power and if the injected voltage is in quadrature with line current it exchanges a reactive power. Therefore, it has the ability to exchange both the real and reactive power in a transmission line [15].

2.4.2.2 Static Synchronous Compensator (STATCOM)

It is designed based on Voltage source converter (VSC) electronic device with Gate turn off thyristor and dc capacitor coupled with a step down transformer tied to a transmission line. It converts the dc input voltage into ac output voltages to compensate the active and reactive power of the system. The STATCOM has better characteristics than SVC and it is used for voltage control and reactive power compensation. STATCOM placed on a transmission network improve the voltage stability of a power system by controlling the voltage in transmission and distribution systems, improves the damping power oscillation in transmission system, and provides the desired reactive power compensation of a power system [15].

2.4.2.3 Unified Power Flow Controller (UPFC)

It is designed by combining the series compensator (SSSC) and shunt compensator (STATCOM) coupled with a common DC capacitor. It provides the ability to simultaneously control all the transmission parameters of power systems, i.e. voltage, impedance and phase angle. it consists of two converters — one connected in series with the transmission line through a series inserted transformer and the other one connected in shunt with the transmission line through a shunt transformer. The DC terminal of the two converters is connected together with a DC capacitor. The series converter control to inject voltage magnitude and phase angle in series with the line to control the active and reactive power flows on the transmission line. Hence the series converter will exchange active and reactive power with the line [15].

CHAPTER THREE

OPTIMAL PLACEMENT AND SIZING OF FACTS CONTROLLERS

3.1 Introduction

In recent times, the application of FACTS controllers is a very effective solution to prevent system collapse due to their fast and very flexible control. The fact that optimization techniques can be readily used to study the system problem has led to formulations that "optimize" a system considering both economic and technical criteria. This chapter discusses optimal placement for improving the voltage profile, as well as reducing real and reactive power losses.

3.2 Optimal placement of FACTS

In power systems, appropriate placement of FACTS is becoming important. Improperly placed FACTS controllers fail to give the optimum performance and can even be counterproductive. Therefore, proper placement of these devices must be examined. This chapter investigates the optimal location of SVC and TCSC controller to get the maximum possible benefit of maximum power transfer and enhance bus voltage under steady state conditions. There are many indices which use the elements of the admittance matrix and some system variables such as bus voltages and power flow through lines such as voltage collapse point indicator (VCPI), Line index (L-index), Line Stability index (L_{mn}), Line Voltage Stability index (LQP), Novel Voltage Stability index (NVSI) and Fast Voltage Stability index (FVSI) [18-20]. Some of these indices use the concept of the maximum power transfer that can be transmitted to the load bus in a simple two bus power system. These indices require less computational effort and are suitable for quickly

diagnosing the power system voltage stability. These indices should be use on-line or off-line to help operators in real time operation of power system or in designing and planning operations. In this dissertation line indices are used to find the optimal location of FACTS controllers. Three different types of indices are used to identify the weakest line in power system network.

3.2.1 Fast Voltage Stability Index (FVSI)

This index can either be referred to a bus or a line. The voltage stability index used in this dissertation refers to a line. Generally, it is started with the current equation to form the power or voltage quadratic equations. The criterion employed in this work was to set the discriminant of the roots of voltage or power quadratic equation to be greater than zero. When the discriminant is less than zero, it causes the roots of the quadratic equations to be imaginary which in turn cause voltage instability in the system. The line index that is evaluated close to 1 will indicate the limit.

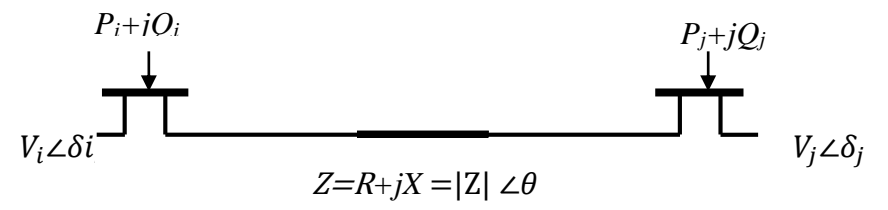


Figure 3.1: Two bus system.

Where:

 V_i , V_j =voltage on sending and receiving end buses.

P_i, Q_i= active and reactive power on the sending end bus

 P_{j} , Q_{j} = active and reactive power on the receiving end bus

 S_{i} , S_{j} = apparent power on the sending and receiving end buses

 $\delta = \delta_i - \delta_j$ (Angle difference between sending and receiving end

$$\overrightarrow{I_{ij}} = \frac{\overrightarrow{v_i} - \overrightarrow{v_j}}{\overrightarrow{z}} \dots \tag{3.1}$$

$$P_j + jQ_j = I_{ji}^* * \vec{V}_j = \vec{V}_j * \frac{\vec{V}_i - \vec{V}_j}{\vec{Z}}.$$
 (3.2)

The imaginary part of Equation (3.2) is the reactive power received at bus j, which can be described as:

$$Q_{j} = \frac{V_{i}V_{j}(R_{ij}\sin\delta + X_{ij}\cos\delta) - X_{ij}V_{j}^{2}}{R_{ij}^{2} + X_{ij}^{2}}.$$
(3.3)

And rewritten as a second-order equation for V_J:

$$V_j^2 - V_i V_j \left(\frac{R_{ij}}{X_{ij}} \sin \delta + \cos \delta\right) + \left(X_{ij} + \frac{R_{ij}^2}{X_{ij}}\right) Q_j = 0.....(3.4)$$

FVSI is based on the principle that the system is stable as long as there are only real solutions to Equation (3.4). In other words, the system is stable as long as the discriminant of Equation (3.4) is not negative:

$$\left[V_i\left(\frac{R_{ij}}{X_{ij}}\sin\delta + \cos\delta\right)\right]^2 - 4\left(X_{ij} + \frac{R_{ij}^2}{X_{ij}}\right)Q_j \ge 0...$$
(3.5)

Simplifying the expression, and assuming that the angle difference, δ , is normally very small ($\delta \approx 0$, $R_{ij} \sin \delta \approx 0$ and $X_{ij} \cos \delta \approx X_{ij}$) gives:

$$(X_{ij}V_i)^2 \ge 4X_{ij}(R_{ij}^2 + X_{ij}^2)Q_j.$$
 (3.6)

FVSI is thus defined as the ratio between the two terms [18]:

$$\frac{4Z_{ij}^{2}Q_{j}}{V_{i}^{2}X_{ij}} = FVSI_{ij} \le 1.$$
(3.7)

Where,

 Z_{ij} = line impedance.

 X_{ij} = line reactance

 Q_{j} = reactive power at the receiving end

 V_i = sending end voltage

3.2.2 Line stability index (LQP)

Line stability index LQP can be obtained from the equation

$$LQP=4\left(\frac{X}{V_{i}^{2}}\right)\left(\frac{X}{V_{i}^{2}}P_{i}^{2}+Q_{j}\right)....(3.8)$$

Where,

X = line reactance

 P_{i} active power at the sending end

 Q_{j} = reactive power at the receiving end

 V_i = sending end voltage

3.2.3 Novel Voltage Stability Index (NVSI)

The index is mathematically formulated as below

$$NVSI = \frac{2X\sqrt{P_j^2 + Q_j^2}}{2XQ_j - |V_i|^2}.$$
(3.9)

Where,

X =line reactance

 P_{i} = active power at the sending end

 Q_{j} = reactive power at the receiving end

V_i = sending end voltage

To maintain a secure condition, FVSI, LQP and NVSI indices should be maintained less than 1. Table 3.1 represent comparison between line indices" FVSI, LQP and NVSI" [18-20].

Table 3.1: comparison of FVSI, LQP and NVSI.

Index	Formulation	Relative Variable	Assumption	Critical value
FVSI	$\frac{4Z_{ij}^{2}Qj}{{V_{i}^{2}X_{ij}}}$	QVZ	$\delta \approx 0$	1.00
LQP	$4\left(\frac{X}{V_i^2}\right)\left(\frac{X}{V_i^2}P_i^2 + Q_j\right)$	PQVX	R/X<<1	1.00
NVSI	$\frac{2X\sqrt{P_j^2 + Q_j^2}}{2XQ_2 - V_1 ^2}$	PQVX	R=0	1.00

3.3 SVC Optimal Placement Criteria

The previous indices FVSI, LQP and NVSI used to find the optimal location for the SVC and TCSC in the system. The weakest bus selected by line indices, the SVC connected to bus bar which gives the best improvement of the system. Equations (2.1 to 2.11) is used to set parameter of SVC to improve the voltage profile at the candidate buses to flat profile. The injected reactive power from SVC is modified adapted until the system reached the desired improvement in the voltage and power losses.

The SVC parameter limits must be set correctly to allow the power flow program to converges toward the solution; if these parameters does not specified correctly, the power flow program will not converges to the solution.

3.4 TCSC Optimal Placement Criteria

Equations (2.12 to 2.19) is used to set parameter of TCSC to reduce the power losses at the candidate lines to minimum power losses in the transmission line. The TCSC installed in the system adopted at the consideration the parameter set far away from the resonance value to avoid problems with control (resonance region limits).

The line having the highest value of line indices is considered the best location for TCSC, followed by other lines having less value. And branches having transformers have not been considered as optimal placement of TCSC. The TCSC's is installed one by one and the system improvements are compared with the previous case until there are no improvement considered.

3.5 Software Development

NEPLAN is one of the most intelligent planning, optimization and simulation tool. It is all operations can be assessed by means of graphical user interfaces (GUIs). In this dissertation, NEPLAN software environment is used to simulate the system and to introduce SVC and TCSC controllers in the system and to obtain the power flow results.

3.5.1 NEPLAN SVC model and parameter

Description of the Model

For Load Flow calculations, a regulated VAR compensator can be described as follows [21]:

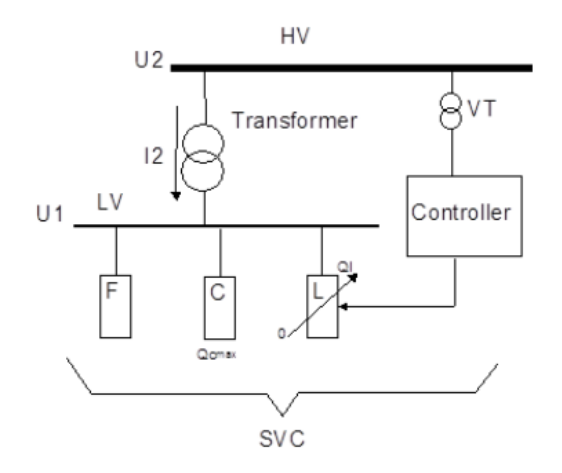


Figure 3.2: NEPLAN Model of a SVC.

F: filter

C: fixed capacitor

L: thyristor controlled reactor

There are three modes:

• Capacitive mode ($V_2 \le Vmin$):

 $I_2 = B_{cap} * V_1$ with $B_{cap} =$ - B_{c0} and $B_{c0} = Qc_{max} \, / \, {V_{2n}}^2; \, Qc_{max} \text{: input value}$

• Inductive mode (V2 >= Vmax):

$$I2 = B_{ind} * V_1 \text{ with } B_{ind} = B_{L0} - B_{c0} \text{ and } B_{L0} = (Q_{cmax} + Q_{Lmax}) / V_{2n}^2$$
;

Q_{cmax}, Q_{Lmax}: input values

• Linear control range, normal mode (Vmin \leq V₂ >= Vmax):

$$I_2 = (V_2 - Vref)/Xsl$$
 for $Xsl \neq 0$; Xsl : input value

$$V_2 = Vref \text{ for } Xsl = 0$$

SVC – Parameters

Name	Name of element.
U ref	Reference voltage for the regulation.
X sl	Slope admittance.
Qc max	Maximum capacitive reactive power in Mvar.
Ql max	Maximum inductive reactive power in Mvar.

3.5.2 NEPLAN TCSC model and parameters

a) Description of the Model

The TCSC consists of a fixed capacitor connected in parallel with a thyristor controlled reactor (TCR) (see Figure 3.3). The TCR is the main control unit of the TCSC: by means of the firing angle of the thyristors, the effective inductive reactance of the TCR varies and causes rapid reactive power exchange between the TCR and the system. Depending on the system conditions, inductive or capacitive vars may be needed. To meet this requirement, the variable inductor is usually connected in parallel with a fixed capacitor. A metal-oxide varistor is also connected in parallel for over-voltage protection [21].

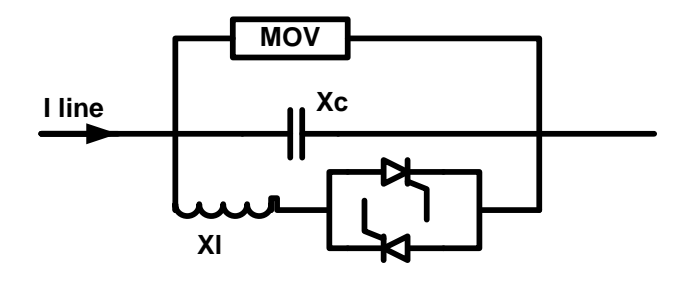


Figure 3.3: Per phase TCSC module.

Firing angles are allowed to vary between 90° and 180° . For a certain firing angle, the variable inductive reactance of the TCR equals to the absolute value of the capacitive reactance of the fixed capacitor X_c , causing a resonance. Thyristors are fired sufficiently far away from the resonance value to avoid problems with control.

A TCSC can either operate in the capacitive or in the inductive region. This means that X_{min} and X_{max} must be entered both as negative (capacitive operation) or both as positive (inductive operation) values [21].

b) TCSC – Parameters

Name	Name of element.
Xc	Reactance of the capacitor in Ohm.
Xl	Reactance of the inductor in Ohm.
X Limits, Theta	Limits on total reactance of the TCSC or on thyristor
Limits	firing angle.
Xmin	Minimum value of module
Xmax	Maximum value of module reactance
Theta min	Minimum value of thyristor firing angle.
Theta max	Maximum value of thyristor firing angle.
Max. Volt. drop	Maximum allowed voltage drop in kV.
Xtot	Control value for total TCSC reactance control in Ohm.

CHAPTER FOUR

SIMULATION AND RESULTS

4.1 Case Study

In this dissertation the case study is a part of National grid of Sudan. This network consists of 82 bus and four voltage levels: 500, 220, 110 and 66 kV which forms the main part of the transmission system in the Sudanese electrical network, Data of the network of the national grid are obtained from the National grid control center. This data is taken at normal load condition the total loading level of the system is 1553.3 MW and 1083.3 MVAr, and the total power generated is 1603.517 MW, 227.008 MVAr. A single line diagram of the partial Sudanese electrical grid is depicted in Figure 4.1.

4.1.1 The National Grid of Sudan

Up to the year 2002, the combined grid-connected generating capacity in Sudan was 728 MW. This was far lower than the required rate and the government decided to increase it to avoid blackouts. The design capacity of generation in the national network amounted to 1234.6 MW up to the end of 2002:

- 342.8 MW which were from hydro generation.
- 180 MW from steam generation.
- 45.2 MW from diesel generation.
- 65 MW from gas generation.
- 450 MW from mixed generation.

At 2006, Construction of Marawe Dam project was intended to roughly double Sudan's power generation in addition to increasing the national network security. Marawe Dam with its peak output of 1260 MW will almost double this capacity if it

runs successfully. The new plant is joined to grid after Marawe Dam. Table 4.1 represent all the plants, types of generation, and total capacity at 2015.

Table 4.1: Generation plant at 2015

Plant	Type of generation	No. of generator Unit	Max. capacity MW					
Marawe	Hydro	10	1260					
Garri	Combined	14	560					
Khartoum North	Steam	6	380					
Kosti	Steam	4	500					
Roseires	Hydro	7	280					
Sennar	Hydro	2	15					
Jabal Aulia	Hydro	8	33					
Kassala	Diesel	1	7.5					
El Girba	Hydro	7	24					
ETH	-	-	100					
	Total capacity							

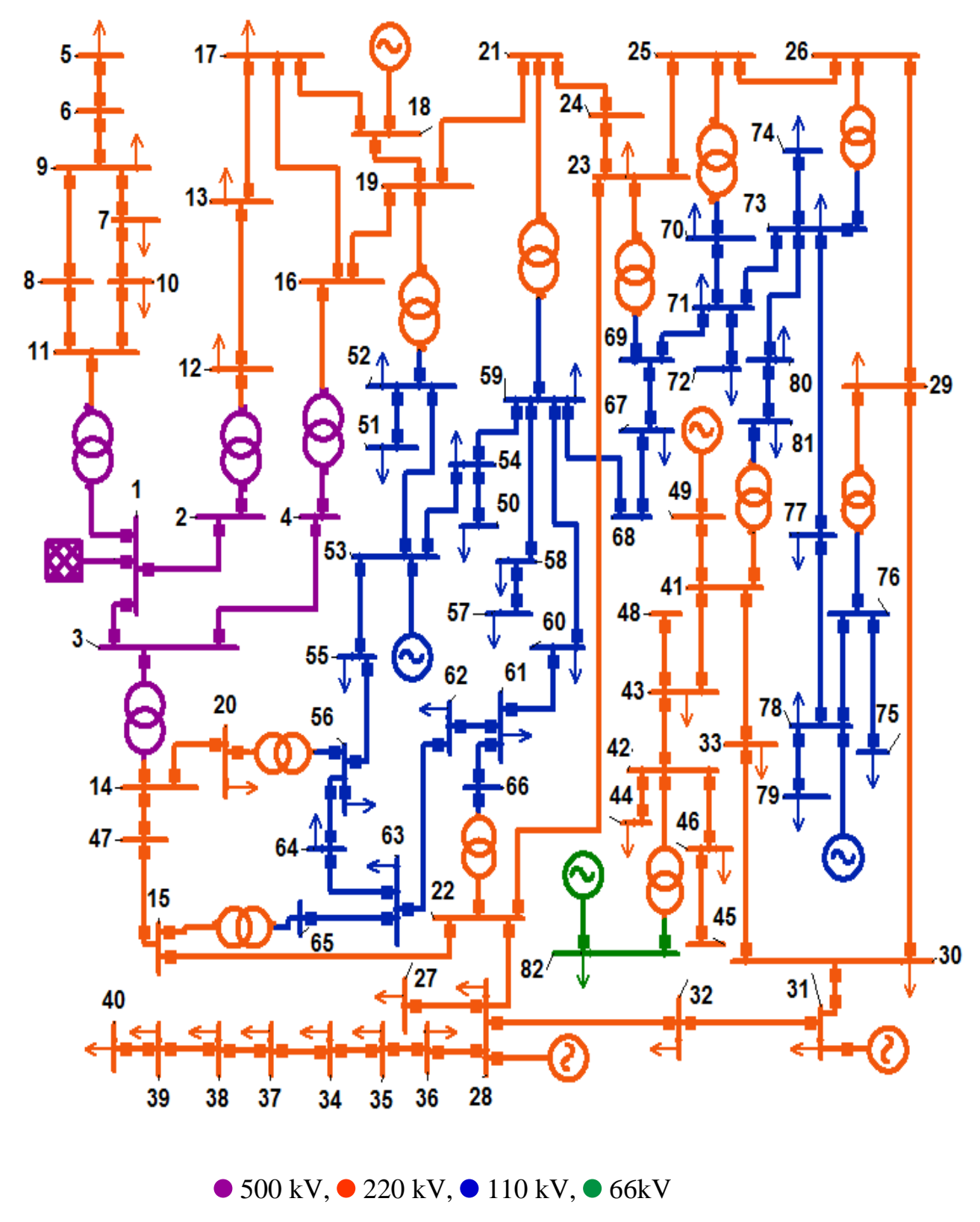


Figure 4.1 single line diagram of Sudanese electrical network.

4.2 System without FACTS controllers

The system is simulate in NEPLAN software environment using the operational data given in appendix. The network operated at normal condition.

Table 4.1 shows the bus voltages and angles at base case and table 4.2 shows the load flow result at base case. In this study Newton-Raphson method was used to obtain the power-flow solution.

Table 4.2: Bus Voltage and angle at base case:

Bus	Bus		Voltage		Bus	Bus		Voltage	
No.	Name	kV	per unit	angle°	No.	Name	kV	per unit	angle °
1	MWP500	500	1	0	42	GRB2	218.15	0.9916	-25
2	ATB5	501.571	1.0031	-3.7	43	SHK2	219.52	0.9978	-24
3	MRK5	488.86	0.9777	-7.6	44	NHLF2	218.11	0.9914	-25
4	KAB5	489.951	0.9799	-8.3	45	ARO2	219.62	0.9982	-25
5	WHL2	217.619	0.9892	-8.7	46	KSL2	219.38	0.9972	-25
6	WWA2	224.494	1.0204	-8	47	HUD	220.04	1.0002	-20
7	DEB2-B1	224.748	1.0216	-6.2	48	UTP2	219.62	0.9983	-24
8	DEB2-B2	229.741	1.0443	-5	49	SHD2	220	1	-23
9	DON2	225.643	1.0256	-7.7	50	KHE1	108.04	0.9821	-27
10	MWT2	226.925	1.0315	-2.8	51	IZB1	106.29	0.9663	-26
11	MWP2	228.452	1.0384	-1.5	52	IBA1	107.08	0.9734	-25
12	ATB2	203.269	0.924	-9.1	53	KHN1	110	1	-26
13	SHN2	213.146	0.9688	-13.8	54	KUK1	108.33	0.9848	-27
14	MRK2	221.126	1.0051	-19.4	55	IZG1	107.25	0.975	-26
15	GAM2	216.561	0.9844	-20.4	56	MHD1	106.06	0.9642	-26
16	KAB2	217.166	0.9871	-16.6	57	FAR1	102.17	0.9288	-27
17	FRZ2	219.471	0.9976	-16.4	58	AFR1	103.01	0.9364	-26
18	GER2	220	1	-16.4	59	KLX1	103.84	0.944	-26
19	IBA2	218.929	0.9951	-18.6	60	LOM1	103.85	0.9441	-26
20	MHD2	220.998	1.0045	-20	61	SHG1	104.68	0.9516	-26
21	KLX2	218.637	0.9938	-19.4	62	MUG`	105.02	0.9547	-27
22	JAS2	215.854	0.9812	-20.8	63	BNT1	105.43	0.9585	-26
23	GAD2	216.286	0.9831	-21	64	OMD1	105.33	0.9576	-26
24	SOB2	218.117	0.9914	-19.8	65	GAM1	108.44	0.9858	-26
25	NHAS2	210.632	0.9574	-23.5	66	JAS1	110.38	1.0035	-25
26	MAR2	210.298	0.9559	-24.2	67	BAG1	101.23	0.9203	-24
27	MSH2	219.127	0.996	-20.6	68	SOB1 B2	102.9	0.9355	-25
28	RBK2	220	1	-20.1	69	GAD B2	101.64	0.924	-24
29	SNJ2	213.631	0.971	-23.7	70	NHAS1	113.84	1.0349	-26
30	SNG2	217.655	0.9893	-23.1	71	OHAS1	113.49	1.0317	-26
31	ROS2	220	1	-18.5	72	GND1	113.12	1.0284	-26
32	RNK2	221.742	1.0079	-19.4	73	MAR1 B1	113.2	1.0291	-27

33	HWT2	219.626	0.9983	-23.7	74	MAN1	112.05	1.0186	-28
34	OBD2	219.71	0.9987	-23.2	75	ORBK1	112.17	1.0197	-25
35	UMR2	221.199	1.0054	-21.6	76	SNJ 1	112.21	1.0201	-25
36	TND2	221.586	1.0072	-21.1	77	HAG1	111.27	1.0116	-26
37	DBT2	220.411	1.0019	-23.9	78	SNP1	110	1	-25
38	ZBD2	220.142	1.0006	-24.1	79	MIN1	104.29	0.9481	-26
39	FUL2	220.571	1.0026	-24.6	80	FAO1	110.54	1.0049	-27
40	BBN2	221.01	1.0046	-24.7	81	GDF 1	111.82	1.0165	-26
41	GDF2	219.615	0.9983	-24.2	82	GRB6	66	1	-26

Table 4.3: Power flow results at base case:

From	To	Line	P	Q	P Loss	Q Loss	Loading
bus	bus	No.	MW	MVAr	MW	MVAr	%
69	67	1	44.524	-4.279	0.2022	0.1612	29.89
6	5	2	14.547	0.568	0.1867	-40.2693	3
7	9	3	21.267	-17.281	0.106	-19.4675	8.28
11	10	4	85.533	7.309	0.373	-3.0979	25.52
12	13	5	143.335	-143.447	3.9588	-31.9876	23.04
11	8	6	44.682	-24.022	0.537	-23.0091	15.08
10	7	7	55.352	-10.089	0.629	-16.7687	16.84
9	6	8	14.577	-26.665	0.0302	-68.8835	3.11
8	9	9	44.145	-1.013	0.4089	-18.3098	13.06
1	2	10	246.304	-150.523	1.6304	-227.912	11.53
1	3	11	684.998	-263.563	9.2555	-604.129	15.16
3	4	12	277.801	-97.047	0.3596	-32.6829	12.03
13	17	13	106.113	-132.075	1.9928	-36.1638	18.36
17	18	14	33.929	-182.002	0.1179	-1.5076	19.48
16	19	15	333.782	-157.923	2.8673	1.2191	39.27
52	51	16	68.208	39.774	0.2017	-0.2175	17.03
52	53	17	84.91	-214.318	1.8548	6.2865	49.72
54	50	18	82.004	53.171	0.0874	0.0436	41.67
56	55	19	36.399	-126.481	0.4105	0.9014	28.66
53	54	20	119.754	255.433	0.5689	4.1539	61.7
53	55	21	39.302	177.206	1.1016	3.2608	38.11
14	20	22	192.848	-41.056	0.5546	-6.1948	20.59
58	57	23	50.427	32.694	0.1614	-0.561	13.47
59	58	24	67.847	41.074	0.2164	-0.0968	17.64
59	54	25	9.157	-170.897	1.7158	6.4934	61
59	60	26	88.699	-25.444	0.0793	0.0529	20.52
60	61	27	3.276	-83.515	0.1679	-0.0219	18.59

61	62	28	22.242	-29.819	0.0456	-0.8095	8.21
63	62	29	53.361	71.598	0.0916	0.0225	19.56
56	64	30	82.377	40.839	0.2351	0.095	20.02
64	63	31	0.83	-13.686	0.0032	-0.5247	3.01
65	63	32	112.875	118.907	1.2724	3.5599	34.92
21	24	33	153.925	26.495	0.1945	-1.6716	24.26
24	23	34	153.73	28.167	0.651	-5.3725	24.33
67	68	35	7.832	-28.676	0.5314	0.1362	59.07
68	59	36	7.3	-28.812	0.2876	0.0593	58.11
66	61	37	85.901	97.463	1.851	3.7283	27.18
22	23	38	22.764	-31.731	0.0294	-13.6741	4.18
23	25	39	127	37.85	1.2962	-15.3411	20.81
71	69	40	12.22	30.333	2.3977	0.4865	57.97
70	71	41	57.355	44.239	0.0681	-0.2566	14.69
71	72	42	27.859	12.823	0.0375	-1.4297	6.24
71	73	43	6.12	-4.525	0.0746	-1.8188	13.49
27	22	44	18.415	2.438	0.1374	-56.7841	1.96
28	27	45	25.455	-14.229	0.0518	-42.201	3.06
25	26	46	43.619	-8.553	0.0898	-13.3328	7.17
73	74	47	10.955	1.737	0.069	-2.321	11.31
29	26	48	27.807	26.037	0.1493	-20.6009	6.06
73	77	49	2.861	11.857	0.1554	-1.0033	21.68
78	77	50	5.091	-10.562	0.2031	-1.7386	21.44
76	78	51	18.419	43.677	0.6251	0.4227	84.98
76	75	52	0.336	-1.788	0.0004	-3.2643	3.26
78	79	53	14.999	8.157	0.6175	-1.3946	31.22
73	80	54	6.699	3.315	0.1263	-2.2482	13.28
30	29	55	63.414	68.531	0.3883	-11.1206	14.57
31	30	56	106.99	-25.893	1.6	-39.8294	16.99
31	32	57	32.677	-55.995	0.1805	-55.3223	6.81
30	33	58	29.946	-60.179	0.173	-34.6115	7.13
28	36	59	44.81	-56.136	0.2436	-43.4277	7.54
35	34	60	39.827	-12.3	0.2737	-24.026	8.7
34	37	61	19.797	-20.052	0.064	-17.4264	5.92
37	38	62	13.483	-6.564	0.0165	-13.0728	3.14
38	39	63	10.106	-17.255	0.0216	-23.6209	4.2
39	40	64	3.364	-13.28	0.0044	-15.7832	2.87
36	35	65	43.558	-18.268	0.1017	-31.0856	4.92

total					50.1895	-1943.18	
15	22	81	90.557	11.059	0.1694	-9.9772	9.73
81	80	80	4.547	-4.236	0.0982	-5.2118	8.67
49	41	79	38	-44.326	0.1984	-76.1212	6.13
19	21	78	354.255	-54.382	1.2541	-0.4641	37.81
18	19	77	219.811	-33.218	2.0254	-15.5831	23.34
43	48	76	0.001	-11.075	0.0006	-11.0751	1.17
17	16	75	56.616	77.43	0.2754	-13.7576	10.09
47	15	74	204.7	147.835	1.2676	-5.8611	26.5
14	47	73	205.094	145.822	0.3937	-2.0127	26.28
42	44	72	12.034	-11.04	0.0051	-19.0608	1.73
46	45	71	0.002	-17.292	0.0023	-17.2922	1.82
41	43	70	42.81	6.018	0.0108	-3.2184	4.55
43	42	69	42.126	7.796	0.1091	-27.0712	4.51
42	46	68	16.729	-43.68	0.0609	-37.0655	4.95
33	41	67	28.227	-26.525	0.0585	-39.346	4.07

Figures (4.2 - 4.5) shows the buses near to the lower limit, power flow losses in the transmission lines and its percentage loading.

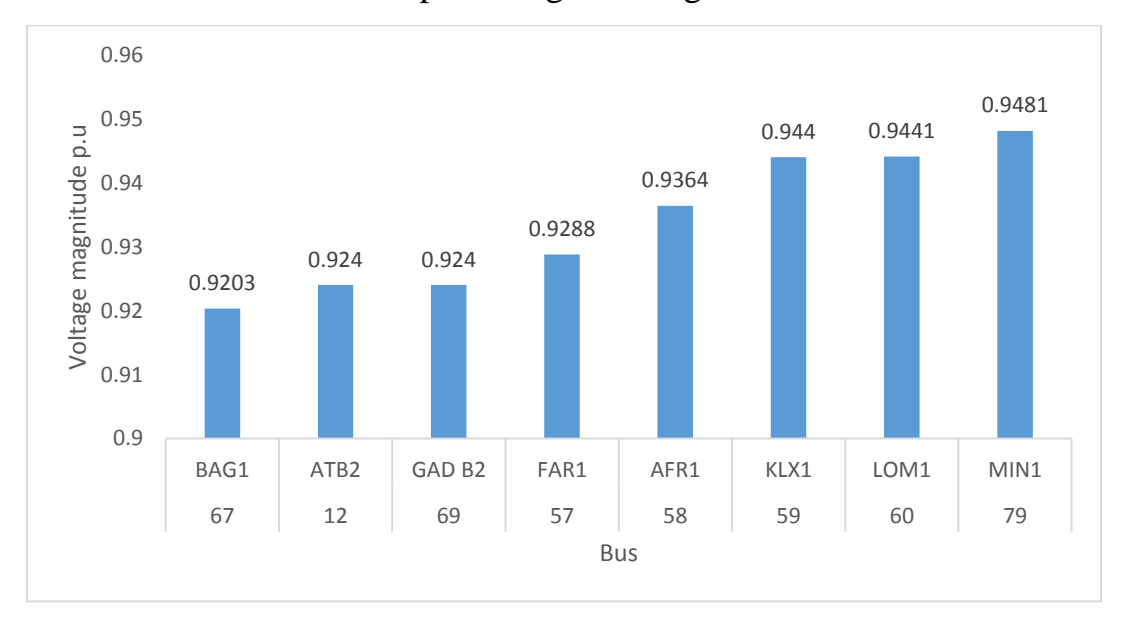


Figure 4.2: Buses near to the lower limit

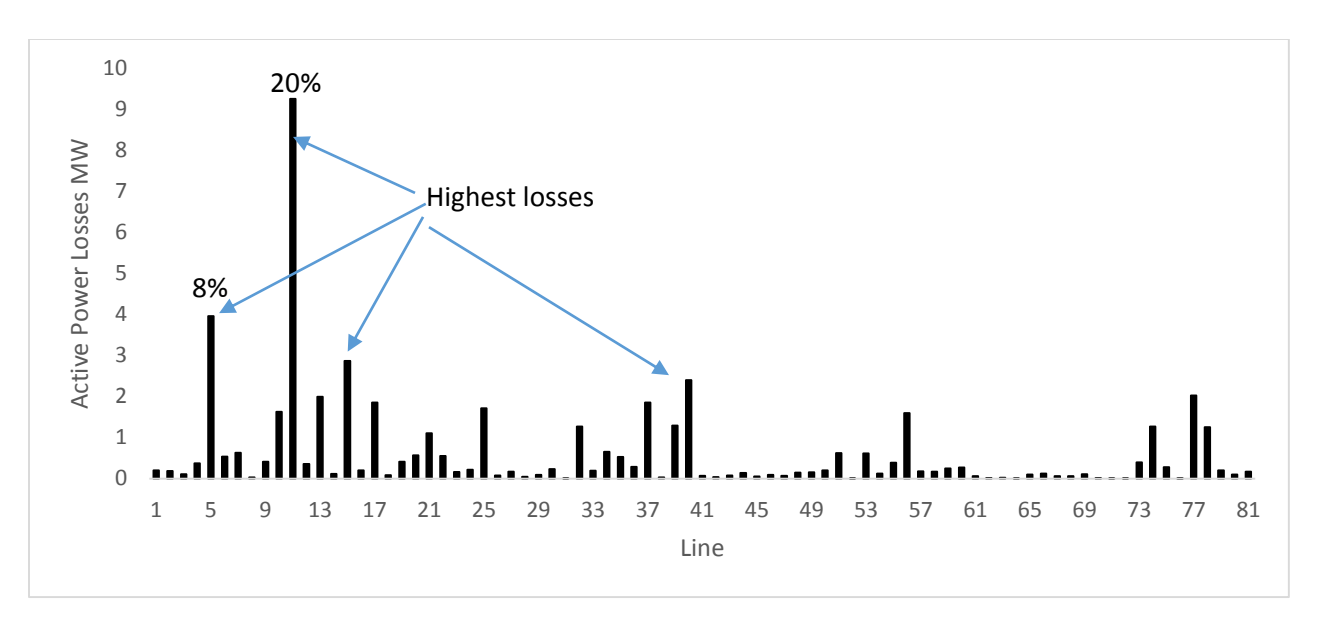


Figure 4.3: Active Power Losses at base case

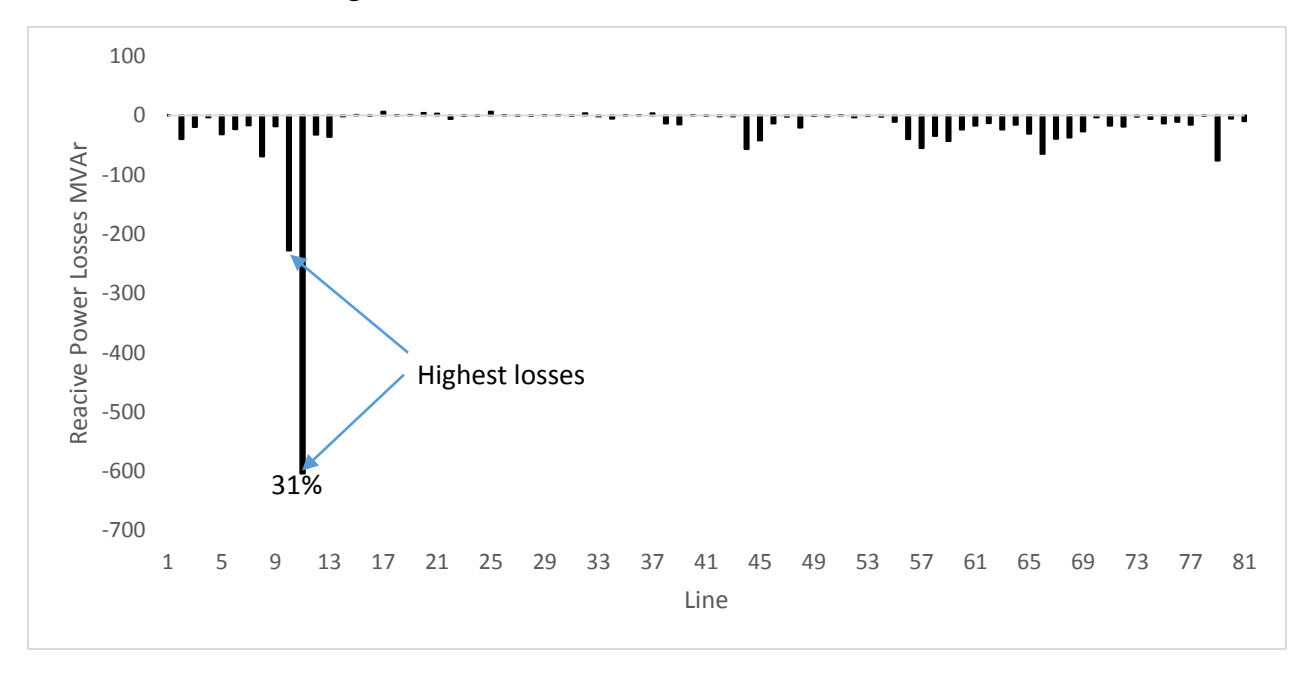


Figure 4.4: Reactive Power Losses at base case

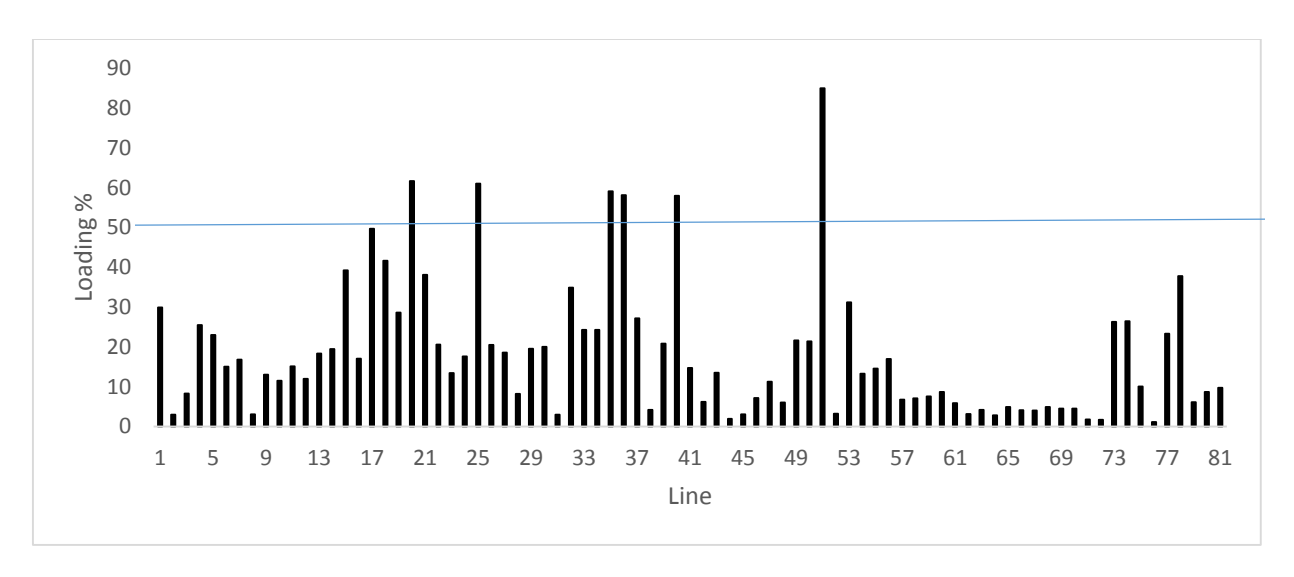


Figure 4.5: Transmission lines Loading.

It can be observed from the results presented in Table 4.2 that all nodal voltages are within accepted voltage magnitude limits (i.e. $100 \pm 10\%$ in the Sudan), the eight buses in the network are near to the lower statutory limit. Figure 4.3 shows these weak buses. The largest power flow takes place in the transmission line 11 (MWP500 - MRK5), Also the transmission line that incurs higher active and reactive power loss. The active and reactive power system loss is 9.2555 MW and -604.129 MVAr respectively, and total active and reactive power loss is found to be 50.1895 MW and -1943.18 MVAr respectively.

The voltage profile enhancement and minimize active power losses by installing FACTS controllers static SVC and TCSC and must be chosen optimal location and sizing of these controllers.

4.3 Optimal Location of FACTS

Line indices is used to identify the best candidate locations for SVC and TCSC installation as discussed in chapter three. The load of the system is increased gradually until reach the collapse point to verify the unstable state. Line indices at different loading conditions are calculated using equations (3.7),(3.8) and (3.9) and the results are tabulated as shown in Table 4.4.

Table 4.4: Line stability indices with system loading.

Branch	From	То		λ = 1			$\lambda = 1.2$	2		$\lambda = 1.3$	3		$\lambda = 1.4$	
No.	Bus	Bus	LQP	NVSIij	FVSI	LQP	NVSIij	FVSI	LQP	NVSIij	FVSI	LQP	NVSIij	FVSI
1	67	69	0.015	0.054	0.012	0.012	0.064	0.008	0.011	0.07	0.0057	0.01	0.0756	0.004
2	6	5	0.183	0.106	0.188	0.198	0.119	0.204	0.207	0.126	0.2123	0.218	0.1352	0.223
3	11	10	0.008	0.031	0.008	0.023	0.039	0.024	0.032	0.044	0.0328	0.04	0.0492	0.042
4	9	7	0.016	0.06	0.013	0.081	0.046	0.087	0.085	0.048	0.0915	0.108	0.1143	0.102
5*	12	13	0.38	0.354	0.532	0.013	0.037	0.019	0.64	0.538	0.9693	0.738	0.6341	1.133
6	10	7	0.007	0.027	0.007	0.021	0.035	0.02	0.029	0.04	0.0278	0.037	0.0448	0.036
7	11	8	1E-04	0.003	0	0.002	0.004	0	0.003	0.005	0	0.004	0.0052	0
8	9	6	0.074	0.041	0.08	0.133	0.141	0.122	0.081	0.097	0.0757	0.09	0.052	0.096
9	9	8	0.083	0.104	0.076	0.057	0.082	0.053	0.161	0.162	0.1475	0.193	0.186	0.175
10	2	1	0.112	0.155	0.1	0.149	0.209	0.123	0.174	0.238	0.138	0.203	0.2699	0.157
11*	1	3	0.14	0.162	0.221	0.256	0.425	0.1	0.384	0.495	0.203	0.204	0.2638	0.269
12*	4	3	0.304	0.315	0.253	0.376	0.43	0.262	0.426	0.497	0.2649	0.489	0.5722	0.266
13	13	17	0.037	0.028	0.042	0.054	0.042	0.061	0.065	0.051	0.0726	0.078	0.0601	0.087
14	18	17	0.013	0.054	0.014	0.056	0.031	0	0.025	0.074	0.0261	0.087	0.0483	0
15	16	19	0.05	0.066	0.058	0.025	0.014	0	0.056	0.095	0.06	0.059	0.1056	0.061
16	52	51	0.088	0.086	0.088	0.281	0.254	0.256	0.118	0.114	0.1162	0.128	0.1239	0.126
17*	53	52	0.602	0.448	0.618	0.702	0.563	0.711	0.761	0.638	0.7654	0.829	0.728	0.826
18	54	50	0.082	0.044	0.083	0.094	0.051	0.095	0.065	0.059	0.0661	0.07	0.0644	0.071
19	55	56	0.097	0.055	0.1	0.158	0.09	0.163	0.196	0.113	0.2016	0.239	0.1401	0.246
20	54	53	0.049	0.045	0.05	0.06	0.054	0.061	0.102	0.055	0.1028	0.11	0.059	0.111
21*	53	55	0.228	0.134	0.235	0.33	0.202	0.341	0.389	0.245	0.4013	0.453	0.2963	0.467
22	14	20	0.021	0.048	0.025	0.024	0.061	0.027	0.025	0.069	0.0272	0.026	0.0773	0.027
23	59	58	0.084	0.044	0.114	0.113	0.06	0.153	0.035	0.033	0.0372	0.039	0.0366	0.041
24	58	57	0.03	0.027	0.031	0.037	0.033	0.038	0.041	0.037	0.0423	0.045	0.0408	0.047
25	59	54	0.034	0.047	0.029	0.032	0.03	0.034	0.13	0.07	0.1763	0.15	0.0812	0.203
26	59	60	0.001	0.005	0	0.035	0.057	0.029	0.004	0.007	0	0.006	0.0083	0
27	60	61	0.024	0.012	0.04	0.019	0.01	0.031	0.015	0.008	0.0254	0.011	0.0061	0.019
28	61	62	0.022	0.014	0.024	0.019	0.014	0.021	0.018	0.014	0.0188	0.015	0.0144	0.017
29	62	63	0.173	0.113	0.18	0.19	0.132	0.197	0.199	0.142	0.2048	0.208	0.1528	0.213
31	56	64	0.084	0.064	0.082	0.121	0.087	0.118	0.142	0.101	0.1385	0.165	0.116	0.161
31*	64	63	0.426	0.271	0.754	0.858	0.752	1.516	1.113	1.252	1.9633	1.397	2.3023	2.462
32	65	63	0.031	0.025	0.04	0.029	0.029	0.037	0.027	0.031	0.0346	0.025	0.0326	0.032
33	21	24	0.022	0.073	0.02	0.045	0.101	0.04	0.059	0.117	0.0537	0.077	0.1356	0.07
34	24	23	0.011	0.033	0.009	0.019	0.046	0.016	0.024	0.053	0.0199	0.03	0.0605	0.025
35*	68	67	0.429	0.297	0.447	0.546	0.4	0.568	0.611	0.464	0.6344	0.682	0.5398	0.706
36	59	68	0.01	0.005	0.017	0.012	0.006	0.02	0.013	0.007	0.0211	0.014	0.007	0.023
37	61	66	0.012	0.009	0	0.012	0.01	0	0.012	0.01	0	0.011	0.0109	0

38	23	22	0.004	0.003	0	0.01	0.024	0	0.007	0.004	0	0.009	0.0053	0
39	23	25	0.011	0.018	0	0.006	0.004	0	0.01	0.027	0	0.009	0.0312	0
40	69	71	0.056	0.041	0.053	0.072	0.038	0.072	0.074	0.039	0.073	0.075	0.0393	0.075
41	71	70	0.099	0.081	0.094	0.107	0.093	0.101	0.112	0.099	0.1045	0.117	0.1059	0.108
42	71	72	0.031	0.033	0.03	0.039	0.042	0.037	0.044	0.047	0.0414	0.049	0.0524	0.046
43	71	73	0.001	0.017	0.001	0.017	0.026	0.016	0.026	0.031	0.0248	0.036	0.0374	0.035
44	22	27	0.008	0.004	0	0.042	0.034	0.055	0.015	0.008	0	0.017	0.0093	0
45	27	28	0.037	0.026	0.061	0.086	0.045	0.143	0.116	0.063	0.1908	0.149	0.084	0.246
46	25	26	0.007	0.017	0.008	0.018	0.031	0.021	0.025	0.039	0.0287	0.034	0.0479	0.038
47	74	73	0.022	0.03	0.021	0.027	0.038	0.026	0.031	0.042	0.0291	0.034	0.0468	0.032
48	26	29	0.031	0.018	0.033	0.138	0.139	0.21	0.049	0.025	0.0515	0.06	0.0309	0.063
49	73	77	0.013	0.011	0.013	0.012	0.013	0.012	0.011	0.014	0.0108	0.004	0.0053	0.004
50	77	78	0.022	0.014	0.022	0.002	0.011	0.002	0.01	0.014	0.0099	0.022	0.0189	0.022
51	76	78	0.072	0.047	0.071	0.046	0.046	0.044	0.03	0.047	0.0283	0.014	0.0503	0.011
52	75	76	0.008	0.004	0.008	0.01	0.005	0.01	0.011	0.006	0.0107	0.012	0.006	0.012
53	78	79	0.01	0.009	0.01	0.011	0.01	0.011	0.012	0.011	0.0122	0.013	0.0119	0.013
54	73	80	0.051	0.027	0.051	0.027	0.015	0.027	0.012	0.008	0.0122	0.01	0.0156	0.01
55	29	30	0.229	0.166	0.368	0.113	0.072	0.113	0.108	0.17	0.1406	0.138	0.0821	0.139
56	30	31	8E-04	0.012	0	0.017	0.017	0.018	0.004	0.013	0	0.005	0.0136	0
57	31	32	0.021	0.123	0.009	0.039	0.093	0.051	0.054	0.079	0.0818	0.07	0.0659	0.113
58	30	33	0.012	0.012	0.013	0.003	0.013	0	0.02	0.02	0.021	0.023	0.0231	0.024
59	28	36	0.023	0.041	0.023	0.027	0.05	0.026	0.051	0.057	0.0513	0.076	0.0684	0.078
60	35	34	0.011	0.019	0.01	0.028	0.026	0.026	0.037	0.031	0.0344	0.046	0.036	0.043
61	34	37	0.003	0.012	0.003	0.01	0.016	0.009	0.017	0.019	0.0165	0.024	0.0226	0.024
62	37	38	0.009	0.01	0.01	0.022	0.017	0.023	0.029	0.02	0.0311	0.037	0.0246	0.04
63	38	39	0.031	0.029	0.052	0.042	0.039	0.07	0.049	0.044	0.0796	0.056	0.0502	0.091
64	39	40	0.021	0.018	0.035	0.027	0.023	0.046	0.031	0.026	0.0518	0.035	0.0297	0.059
65*	36	35	0.097	0.145	0.089	0.26	0.228	0.264	0.349	0.284	0.3572	0.442	0.3521	0.455
66	28	32	0.016	0.01	0.016	0.017	0.01	0.017	0.017	0.009	0.0166	0.017	0.0089	0.017
67	33	41	0.034	0.029	0.035	0.023	0.036	0.023	0.016	0.041	0.0158	0.009	0.0464	0.007
68	42	46	0.075	0.093	0.114	0.008	0.007	0.008	0.045	0.113	0.0543	0.034	0.1214	0.034
69	41	43	0.011	0.03	0.017	0.149	0.159	0.221	0.013	0.04	0.0193	0.014	0.044	0.019
70	43	42	0.053	0.043	0.055	0.05	0.048	0.051	0.049	0.051	0.0493	0.047	0.0537	0.047
71	42	44	0.007	0.006	0.006	0.226	0.13	0.234	0.009	0.008	0.0083	0.01	0.0088	0.009
72	46	45	0	0	0	0	0	0	0	0	0	0	0	0
73	14	47	0.013	0.016	0	0.008	0.021	0	0.005	0.024	0	0.001	0.0271	0
74	47	15	0.35	0.363	0.285	0.325	0.445	0.173	0.311	0.488	0.0989	0.294	0.5339	0.007
75	16	17	0.014	0.01	0	0.141	0.134	0.146	0.033	0.018	0	0.041	0.0217	0
76	43	48	0	0	0	0	0	0	0	0	0	0	0	0
77	18	19	0.035	0.018	0	0.013	0.066	0.011	0.07	0.039	0	0.039	0.082	0.044
78	19	21	0.033	0.113	0.026	0.022	0.144	1E-03	0.041	0.164	0.0174	0.063	0.185	0.036

79	41	49	0.172	0.142	0.173	0.231	0.205	0.222	0.269	0.242	0.2525	0.317	0.2872	0.29
80	81	80	0.006	0.009	0.006	0.013	0.011	0.013	0.017	0.012	0.0166	0.021	0.0144	0.021
81	22	15	9E-04	0.016	8E-04	0.014	0.027	0.018	0.024	0.033	0.0302	0.035	0.0408	0.045
82	25	70	0.01	0.009	0	0.012	0.011	0	0.012	0.011	0	0.013	0.0123	0
83	59	21	0.025	0.024	0.027	0.002	0.006	0	0.036	0.063	0.0289	0.037	0.069	0.029
84	52	19	0.24	0.204	0.227	0.108	0.104	0.107	0.307	0.284	0.2749	0.339	0.3172	0.297
85	12	2	0.004	0.007	0	0.004	0.009	0	0.004	0.011	0	0.004	0.0122	0
86	16	4	0.108	0.096	0.115	0.053	0.085	0.059	0.165	0.158	0.1676	0.195	0.1865	0.195
87	3	14	1.42	1.343	0.573	1.982	1.602	0.429	2.355	1.708	0.3284	2.808	1.7938	0.2
88	41	81	0.097	0.125	0.142	0.549	0.462	0.815	0.177	0.178	0.2623	0.206	0.1989	0.306
89	42	82	0.241	0.138	0.25	0.055	0.106	0.075	0.217	0.125	0.2245	0.208	0.12	0.215
90	26	73	0.119	0.115	0.185	0.042	0.022	0.045	0.148	0.152	0.2232	0.159	0.1654	0.236
91	69	23	0.07	0.038	0.069	0.054	0.048	0.051	0.054	0.053	0.0504	0.054	0.0573	0.05
92	29	76	0.093	0.067	0.092	0.152	0.163	0.225	0.125	0.077	0.1253	0.058	0.1823	0.044
93	56	20	0.001	0.006	0	0.003	0.008	0	0.004	0.009	0	0.005	0.0104	0
94	15	65	0.048	0.04	0.053	0.046	0.045	0.05	0.045	0.048	0.0482	0.043	0.0518	0.045
95	1	11	0.194	0.35	0.088	0.167	0.211	0.24	0.183	0.237	0.2528	0.522	0.5822	0.314
96	22	66	0.042	0.031	0.056	0.012	0.006	0	0.041	0.036	0.0543	0.041	0.0375	0.053

From Table 4.4, it is observed that value of Line index is varying between 0 and 1. Based on this value, it is possible to identify the weakest element. The higher values for Line indices are indicative of most critical buses. Table 4.5 represents the most severe lines in the system which are the candidate locations for SVC and TCSC installation.

Table 4.5 Ranking of lines severity

Rank	Line No.	Line name	LQP	NVSI	FVSI
1	31	OMD_BNT	1.397	2.3023	2.462
2	5	ATB-SHN	0.738	0.6341	1.133
3	17	IBA-KHN1	0.829	0.728	0.826
4	35	SOB_BAG	0.682	0.5398	0.706
5	21	KHN_IZG	0.453	0.2963	0.467
6	65	TND_UMR	0.442	0.3521	0.455
7	11	MWP_MRK	0.204	0.2638	0.269
8	12	MRK_KAB	0.489	0.5722	0.266

4.4 System after incorporation SVC Controller:

According to the obtaining results, the optimal location chosen to install SVC. SVC controller can be connected at buses or midpoint of transmission line, four SVC are installed. SVC controllers are connected to buses 64, 12, 52, and 67. The setting of SVC represented in table 4.6.

Table 4.6: Parameters of installed SVC

Element	Bus	Vref %	Xsl	Qcmax MVAr	Qlmax MVAr	Q injected
SVC-1	OMD	100	5	210	50	-184.823
SVC-2	ATB	100	5	130	30	-115.268
SVC-3	IBA	100	5	250	80	-236.779
SVC-4	BAG	100	5	150	40	-121.363

Table 4.7 and Table 4.8 show the power flow result after installing the SVC. Table 4.7: Bus voltage and angle after installing SVC:

Bus	Bus	Volt	age	Bus	Bus	Vol	tage
		Magn	itude			Magr	nitude
No.	Name	without	with	No.	Name	without	with
		SVC	SVC			SVC	SVC
1	MWP500	1	1	42	GRB2	0.9916	0.9937
2	ATB5	1.0031	1.0134	43	SHK2	0.9978	1.0003
3	MRK5	0.9777	0.9812	44	NHLF2	0.9914	0.9935
4	KAB5	0.9799	0.9834	45	ARO2	0.9982	1.0004
5	WHL2	0.9892	0.9843	46	KSL2	0.9972	0.9994
6	WWA2	1.0204	1.0093	47	HUD	1.0002	1.0201
7	DEB2-B1	1.0216	1.0062	48	UTP2	0.9983	1.0008
8	DEB2-B2	1.0443	1.0293	49	SHD2	1	1
9	DON2	1.0256	1.0123	50	KHE1	0.9821	0.9892
10	MWT2	1.0315	1.0151	51	IZB1	0.9663	0.993
11	MWP2	1.0384	1.0219	52	IBA1	0.9734	1
12	ATB2	0.924	1	53	KHN1	1	1
13	SHN2	0.9688	1.0035	54	KUK1	0.9848	0.9918
14	MRK2	1.0051	1.0247	55	IZG1	0.975	0.9919

15	GAM2	0.9844	1.0054	56	MHD1	0.9642	0.9922
16	KAB2	0.9871	0.9904	57	FAR1	0.9288	0.964
17	FRZ2	0.9976	0.9993	58	AFR1	0.9364	0.9713
18	GER2	1	1	59	KLX1	0.944	0.9786
19	IBA2	0.9951	0.9997	60	LOM1	0.9441	0.9783
20	MHD2	1.0045	1.0248	61	SHG1	0.9516	0.9846
21	KLX2	0.9938	0.9988	62	MUG`	0.9547	0.9924
22	JAS2	0.9812	1.0021	63	BNT1	0.9585	0.9977
23	GAD2	0.9831	1.0024	64	OMD1	0.9576	1
24	SOB2	0.9914	0.9996	65	GAM1	0.9858	1.0223
25	NHAS2	0.9574	0.9842	66	JAS1	1.0035	1.014
26	Mar2	0.9559	0.9721	67	BAG1	0.9203	1
27	MSH2	0.996	1.0049	68	SOB1 B2	0.9355	0.9863
28	RBK2	1	1	69	GAD B2	0.924	0.9954
29	SNJ2	0.971	0.9801	70	NHAS1	1.0349	1.0005
30	SNG2	0.9893	0.9954	71	OHAS1	1.0317	1.0008
31	ROS2	1	1	72	GND1	1.0284	0.9974
32	RNK2	1.0079	1.0079	73	MAR1 B1	1.0291	1.0284
33	HWT2	0.9983	1.0027	74	MAN1	1.0186	1.0179
34	OBD2	0.9987	0.9987	75	ORBK1	1.0197	1.0216
35	UMR2	1.0054	1.0054	76	SNJ 1	1.0201	1.0219
36	TND2	1.0072	1.0072	77	HAG1	1.0116	1.0112
37	DBT2	1.0019	1.0019	78	SNP1	1	1
38	ZBD2	1.0006	1.0006	79	MIN1	0.9481	0.9495
39	FUL2	1.0026	1.0026	80	FAO1	1.0049	1.0052
40	BBN2	1.0046	1.0046	81	GDF 1	1.0165	1.0185
41	GDF2	0.9983	1.0008	82	GRB6	1	1

Table 4.8: Power flow results after installing SVC:

Line	Fro m	То	P	Q	P Loss	Q Loss	Loadi ng%	Loading %
Number	bus	bus	\mathbf{MW}	Mvar	MW	Mvar	with	without
1*	69	67	-62.78	97.004	0.2528	-1.297	71.35	29.89
2	6	5	14.495	-4.141	0.1552	-39.8427	3.14	3
3	7	9	-21.097	-0.186	0.1148	-18.8635	6.43	8.28
4	11	10	85.509	6.857	0.3844	-2.8775	25.92	25.52
5*	12	13	104.124	-56.314	3.9588	-50.7106	12.43	23.04
6	11	8	44.718	-24.524	0.5208	-22.1068	15.41	15.08
7	10	7	55.317	-10.761	0.6489	-16.0451	17.14	16.84

8	9	6	14.52	-30.659	0.0247	-67.2632	3.52	3.11
9	8	9	-43.743	-15.302	0.0247	-17.7193	14.13	13.06
10*	1	2	-205.462	-46.27	1.6304	-134.18	8.3	11.53
11	1	3	717.805	-280.64	10.092	-573.317	15.92	15.16
12	3	4	-277.875	64.518	0.3583	-32.9552	11.59	12.03
13*	13	17	69.731	-26.219	1.6851	-24.257	7.79	18.36
14*	17	18	-15.333	55.318	0.1018	-1.3371	6.03	19.48
15	16	19	318.114	-169.21	2.7073	0.4055	38.19	39.27
16	52	51	68.197	39.674	0.1909	-0.3182	16.56	17.03
17	52	53	-110.446	27.834	1.4321	0.5434	23.91	49.72
18	54	50	82.003	53.161	0.0862	0.0342	41.37	41.67
19	56	55	-41.838	6.298	0.3404	-0.6195	8.96	28.66
20	53	54	-153.684	-124.56	0.4838	1.9093	43.62	61.7
21	53	55	32.478	52.19	1.1276	-0.6695	12.91	38.11
22	14	20	199.548	-55.731	0.5878	-6.3987	21.23	20.59
23	58	57	50.416	32.554	0.1597	-0.7006	12.97	13.47
24	59	58	67.819	40.798	0.2006	-0.233	16.98	17.64
25	59	54	-26.881	-50.923	0.1789	-0.2442	19.8	61
26	59	60	16.226	3.802	0.0793	-0.0755	3.58	20.52
27	60	61	-69.121	-53.94	0.1725	-0.0533	18.82	18.59
28	61	62	14.81	-66.916	0.0453	-0.4837	14.61	8.21
29	63	62	-60.802	-109	0.106	0.2928	26.4	19.56
30	56	64	83.565	-94.937	0.4161	0.7605	26.76	20.02
31	64	63	1.837	34.695	0.0201	-0.504	7.29	3.01
32	65	63	119.357	107.57	1.1365	2.8916	33	34.92
33	21	24	221.889	-63.007	0.4174	-0.5256	35.65	24.26
34	24	23	221.472	-62.481	0.9588	-1.8659	35.54	24.33
35	67	68	-25.932	-0.27	0.4579	-0.1475	48.09	59.07
36	68	59	-25.733	-0.345	0.2989	-0.0749	48.09	58.11
37	66	61	-149.018	-27.03	2.0438	6.3452	32.29	27.18
38	22	23	22.404	-10.248	0.0127	-14.3119	2.58	4.18
39	23	25	133.284	16.868	1.2492	-16.6548	20.69	20.81
40	71	69	-13.62	8.65	2.2335	-1.7412	29.64	57.97
41	70	71	-74.933	22.855	0.085	-0.1559	16.43	14.69
42	71	72	27.861	12.927	0.0399	-1.3263	6.44	6.24
43	71	73	21.73	-31.254	0.0909	0.8114	69.56	13.49
44	27	22	-20.571	-31.136	0.1434	-58.905	3.91	1.96
45	28	27	-27.603	2.235	0.0974	-42.3977	2.89	3.06
46	25	26	32.288	38.66	0.1007	-13.6909	7.9	7.17
47	73	74	-10.886	-4.058	0.0692	-2.3172	11.98	11.31
48	29	26	-26.616	-28.064	0.1493	-21.5854	6.14	6.06
49	73	77	3.623	10.957	0.1545	-1.0209	20.52	21.68
50	78	77	-4.111	7.941	0.1635	-1.7857	16.17	21.44
51	76	78	17.749	49.714	0.672	0.5998	94.46	84.98
52	76	75	-0.336	-1.476	0.0004	-3.276	2.71	3.26
53	78	79	14.999	8.157	0.6175	-1.3946	31.22	31.22

	,							
54	73	80	6.998	2.675	0.124	-2.2499	13.32	13.28
55	30	29	-61.236	-66.812	0.3314	-11.7857	14.27	14.57
56	31	30	-103.167	-6.656	1.5445	-40.4186	16.03	16.99
57	31	32	34.956	-56.486	0.1781	-55.2507	6.97	6.81
58	30	33	29.601	-53.955	0.1577	-35.1276	6.49	7.13
59	28	36	44.81	-56.136	0.2436	-43.4277	7.54	7.54
60	35	34	39.827	-12.3	0.2737	-24.026	8.7	8.7
61	34	37	19.797	-20.052	0.064	-17.4264	5.92	5.92
62	37	38	13.483	-6.564	0.0165	-13.0728	3.14	3.14
63	38	39	10.106	-17.255	0.0216	-23.6209	4.2	4.2
64	39	40	3.364	-13.28	0.0044	-15.7832	2.87	2.87
65	36	35	43.558	-18.268	0.1017	-31.0856	4.92	4.92
66	32	28	-34.214	-41.069	0.1306	-64.6892	5.61	4.12
67	33	41	27.917	-19.785	0.0537	-39.6417	3.58	4.07
68	42	46	16.729	-43.915	0.0612	-37.2256	4.96	4.95
69	43	42	42.13	9.643	0.1128	-27.1844	4.54	4.51
70	41	43	42.814	7.793	0.011	-3.2343	4.56	4.55
71	46	45	0.002	-17.367	0.0023	-17.3671	1.82	1.82
72	42	44	12.034	-11.122	0.005	-19.1431	1.73	1.73
73	14	47	229.932	128.94	0.4152	-2.0693	27.01	26.28
74	47	15	229.517	131.01	1.1296	-6.0682	27.2	26.5
75	17	16	-40.239	-80.815	0.1879	-14.1825	9.57	10.09
76	43	48	0.001	-11.13	0.0006	-11.1304	1.17	1.17
77	18	19	201.333	-56.506	1.8659	-16.7334	21.95	23.34
78	19	21	294.571	-50.384	1.1733	-2.0859	31.38	37.81
79	49	41	-37.791	-27.285	0.2086	-76.2749	4.89	6.13
80	81	80	4.227	-3.631	0.0982	-5.2449	7.76	8.67
81	15	22	-108.6	-18.478	0.2308	-10.1644	11.54	9.73
total					48.618	-1847.4		
							-	

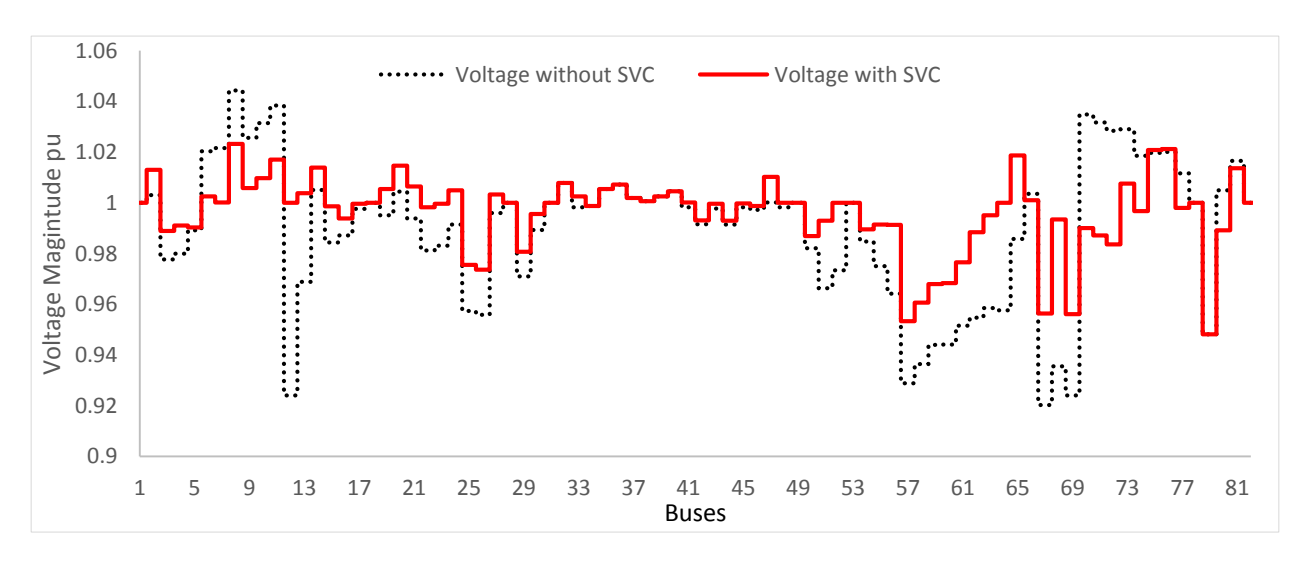


Figure 4.6: Voltage magnitude with and without SVC.

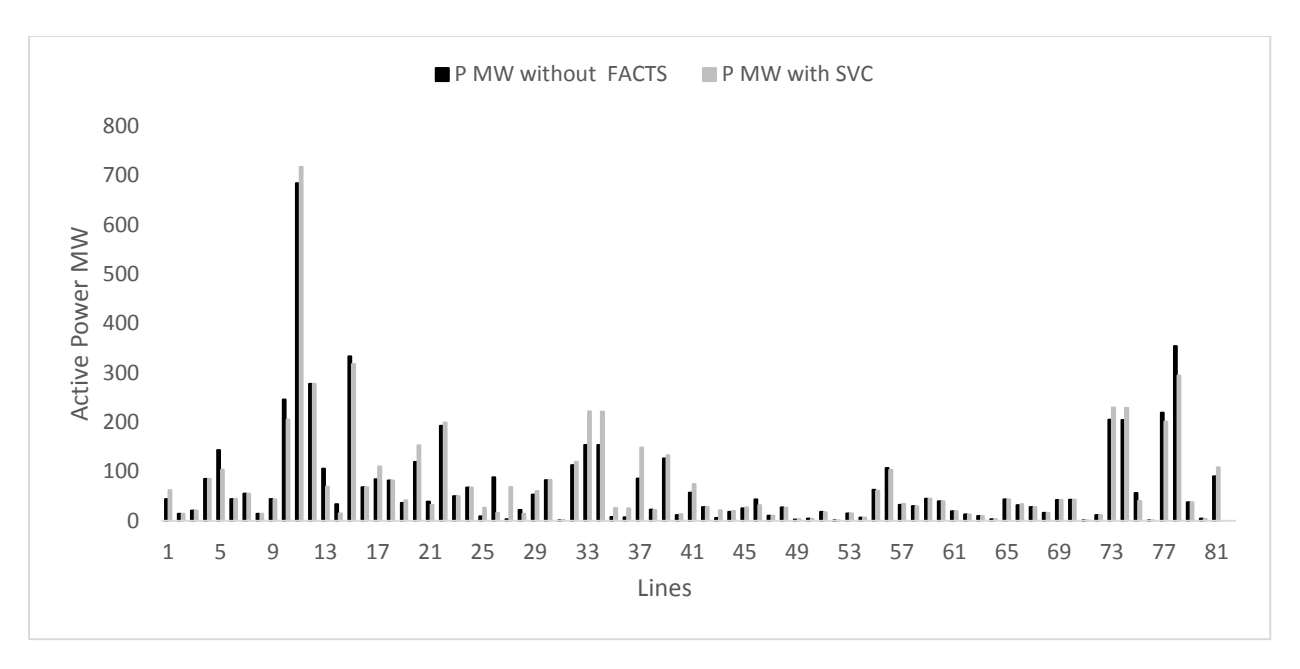


Figure 4.7: Active power without and with SVC.

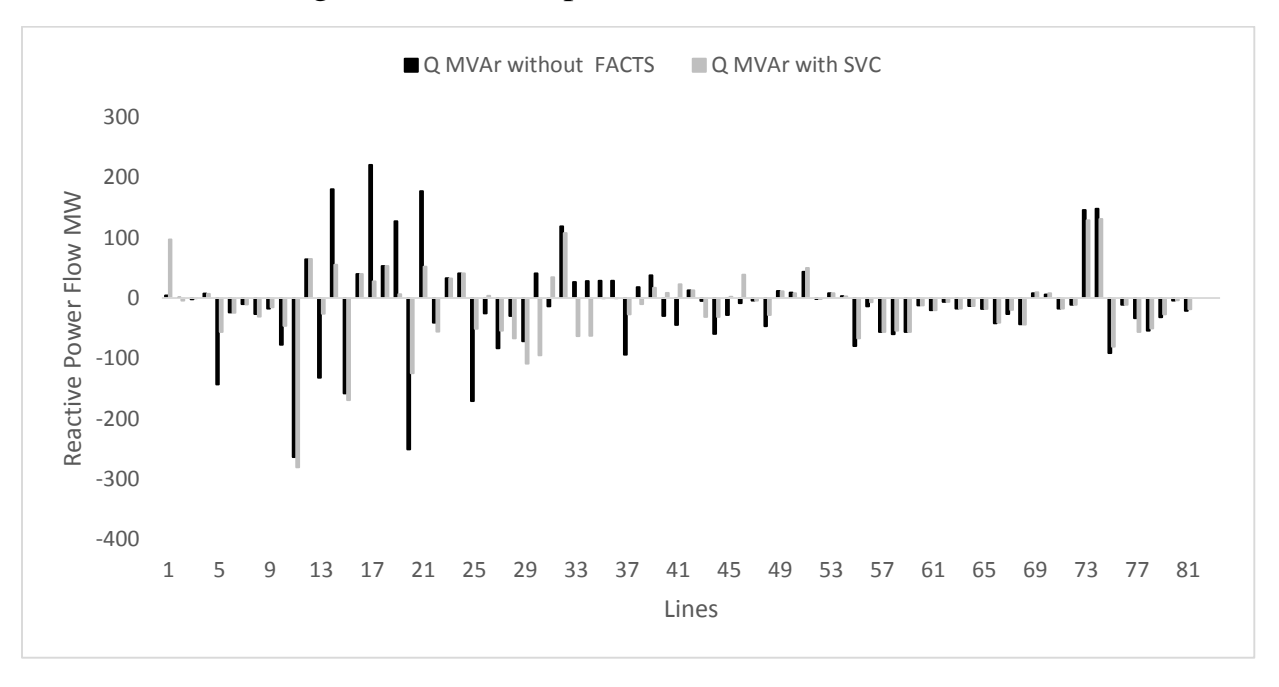


Figure 4.8: Reactive power without and with SVC

Table 4.5 illustrate voltage magnitude at base case and after installation SVC. The SVC injects VAR into selected weakest bus and keeps the nodal voltage magnitude at 1 p.u. The action of the SVC results in an overall improved voltage profile the improvement is clearly appears in Figure 4.6.

Figure 4.7 and Figure 4.8 represent the active and reactive power flow in the line. The SVC generates reactive power in excess of the local demand compared with the base case, there is an increase of reactive power export to near bus this cause increased the power flow in the nearest lines from the location of SVC. The highest active and reactive power flow in line 11 which are 717.805 MW and 280.644 MVAr, power flow increased compared with the base case and also the flow of the reactive power of eight lines has been change to the opposite direction (30, 31, 33, 34, 37, 40, 41 and 46) due to injected VAR from SVC.

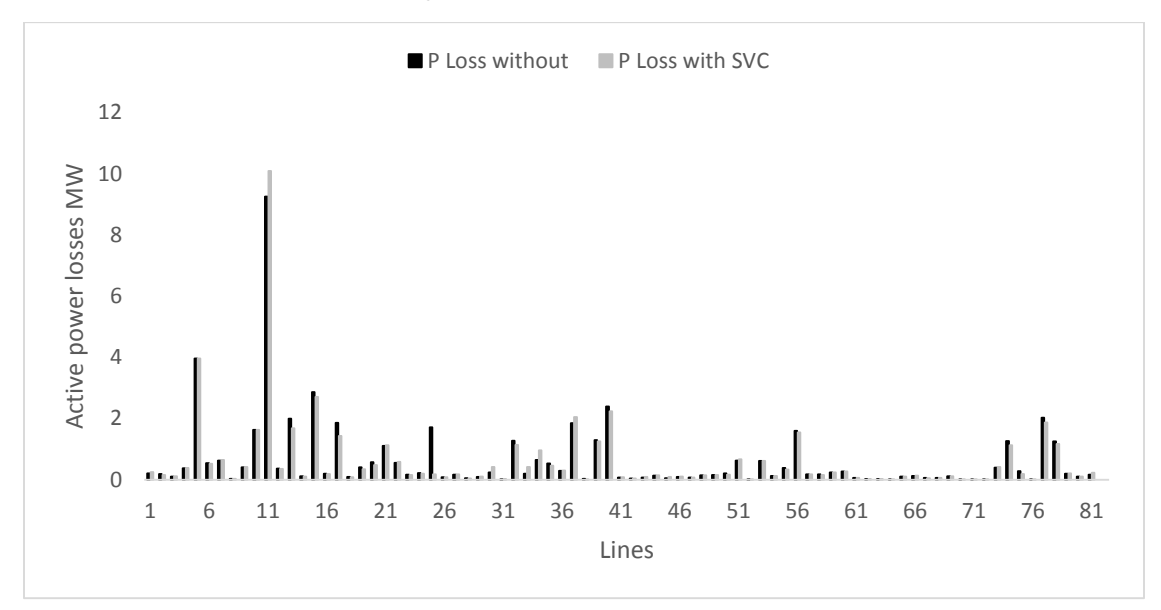


Figure 4.9: Active power Losses with and without SVC.

Figure 4.9 represent active power Losses with and without SVC, we observed the active power losses increased in lines 1, 11, 30, 33, 34, 37 and 51 due to the flow in these lines are increased and decrease in other lines. The total active power losses are decrease to 48.618 MW.

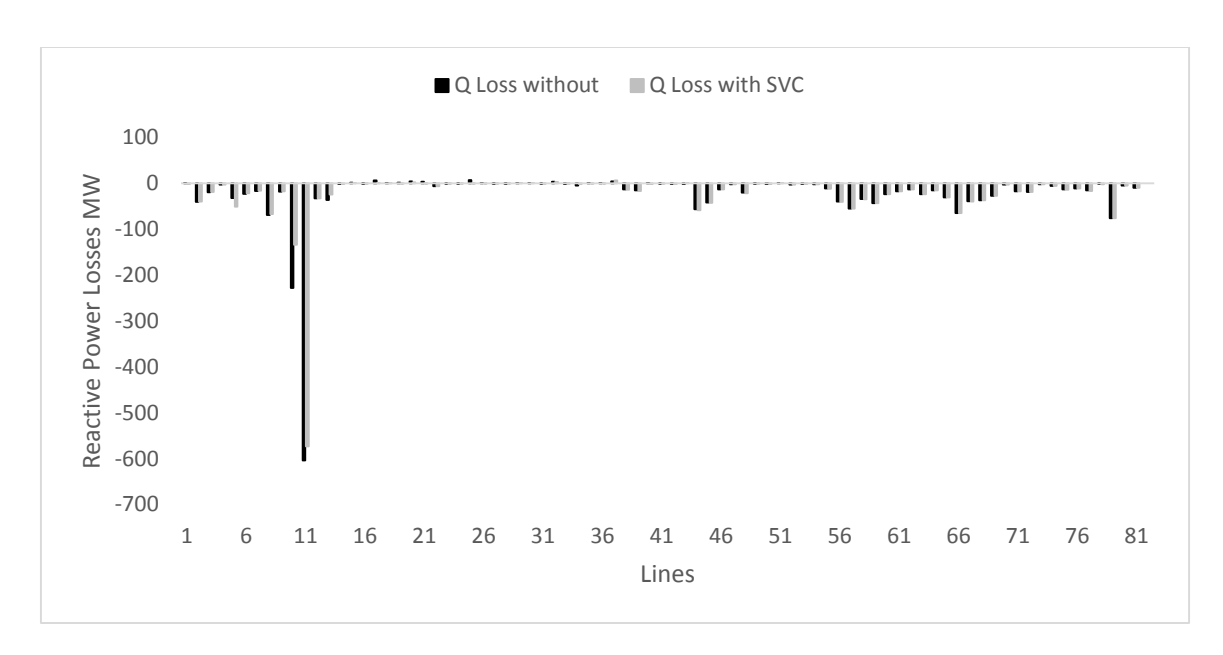


Figure 4.10: Reactive power Losses with and without SVC.

It can be observed from the results presented in Figure 4.10 the reactive power losses increased in lines 2, 5 and 44 and decrease in the other lines. The total reactive power losses are decrease to -1847.4 MVAR compare with base case.

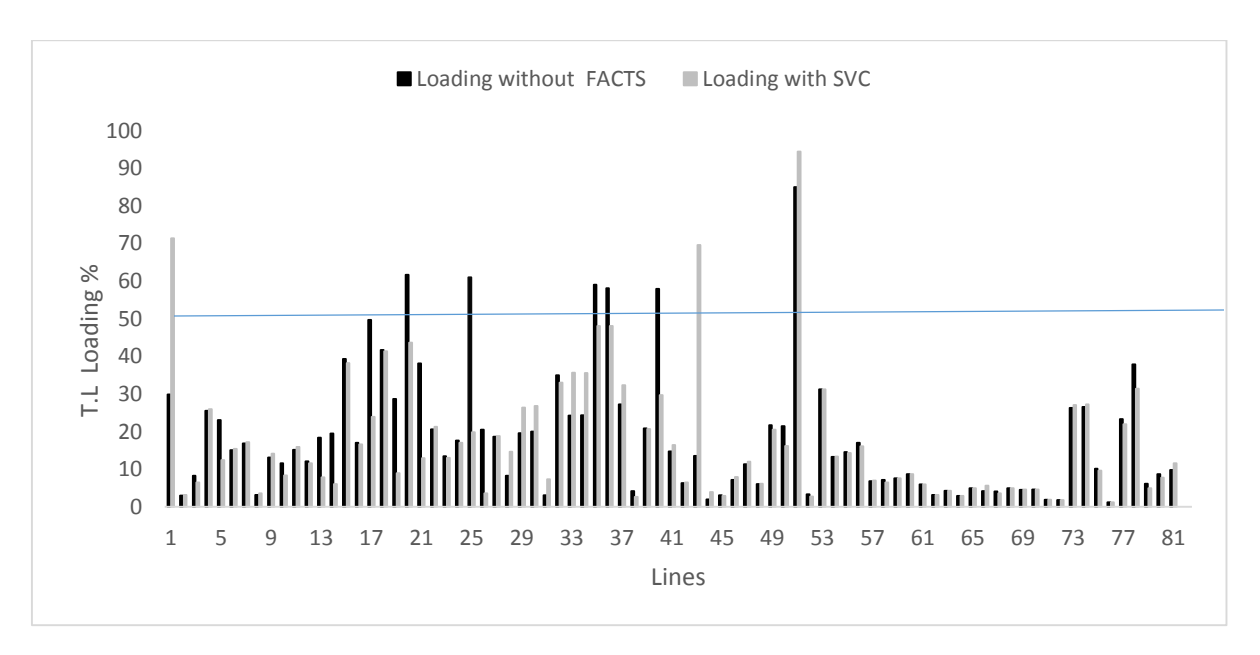


Figure 4.11: Transmission lines loading without and with SVC.

It can be observed from Figure 4.11, only three lines are loaded above 50% of its maximum loading rate. The loading of thirteen lines increase compare with

loading in base case, and the others line is decreased after installing the SVC controllers. The overall loading of the system has been decreased by 5.96 % of the base case loading.

4.5 System after incorporation TCSC Controller:

According to Table 4.5 the seven TCSC module are connected with the lines to minimize active power losses, number of TCSC selected according to the reduction in active power losses. Table 4.9 represented the setting of TCSC.

Table 4.9: Parameters of installed TCSC

From	ТО	Name	Хс	ΧI	Theta min	Theta max	Xmin	Xmax	Xtot set	X _{TCSC}
bus	bus		Ohm	Ohm			Ohm	Ohm	Ohm	%Xij
64	63	TCSC-1	0.7	0.207	90	180	-2	1	-0.2	-24.8%
12	13	TCSC-2	21.14	7.05	90	180	-25	8	-2.278	-10.8%
52	53	TCSC-3	1.3	0.43	90	180	-2	1	-0.3228	-20%
67	68	TCSC-4	6	1.5156	90	180	-7	2	-1.0345	-13.7%
53	55	TCSC-5	1	0.43	90	180	-3	1	-0.2591	-10.7%
36	35	TCSC-6	8.425	2.8	90	180	-9	3	-2.10627	-20%
1	3	TCSC-7	38.2	13.5	90	180	-40	15	-15	-31.4%

Table 4.10: Power Flow after installing TCSC controllers:

Line	From	To	Р	P MW	Q	P Loss	Q Loss	Loading	Loading
Number	bus	bus	MW	without	Mvar	MW	TCSC	TCSC	without
1	69	67	-43.561	-43.561	5.634	0.1963	0.154	29.45	29.89
2	6	5	14.547	14.547	0.568	0.1867	-40.2693	3	3
3	7	9	-21.161	-21.161	-2.186	0.106	-19.4675	6.4	8.28
4	11	10	85.533	85.533	7.309	0.373	-3.0979	25.52	25.52
5*	12	13	129.903	128.436	-146.88	3.3581	-31.0828	21.1	23.04
6	11	8	44.802	44.682	-24.022	0.537	-23.0091	15.08	15.08
7	10	7	55.352	55.352	-10.089	0.629	-16.7687	16.84	16.84
8	9	6	14.578	14.577	-26.665	0.0302	-68.8835	3.11	3.11
9	8	9	-43.736	-43.736	-17.297	0.4089	-18.3098	14.16	13.06
10	1	2	-229.77	-229.77	-71.894	1.4531	-230.195	9.57	11.53
11*	1	3	697.84	696.724	-310.97	8.0121	-578.7	13.14	15.16
12*	3	4	-290.6	-290.47	80.378	0.309	-31.7672	12	12.03
13	13	17	91.814	91.814	-131.94	1.7554	-37.057	17.44	18.36
14	17	18	-29.64	-29.64	192.548	0.1327	-1.4481	20.45	19.48
15	16	19	336.869	336.869	-166.06	2.9735	1.7202	39.99	39.27
16	52	51	68.206	68.206	39.762	0.2003	-0.2302	16.97	17.03

17*	52	53	-90.933	-90.623	227.971	0.6895	6.9069	42.2	49.72
18	54	50	82.004	82.004	53.171	0.0874	0.0436	41.67	41.67
19	56	55	-30.909	-30.909	137.531	0.463	1.1091	28.28	28.66
20	53	54	-121.53	-121.53	-251.56	0.5741	4.1949	62.04	61.7
21*	53	55	45.731	45.5	187.906	1.2434	3.7937	33.693	38.11
22	14	20	191.676	191.676	-46.125	0.5573	-6.1355	20.65	20.59
23	58	57	50.428	50.428	32.695	0.1615	-0.56	13.48	13.47
24	59	58	67.847	67.847	41.076	0.2165	-0.0959	17.64	17.64
25	59	54	6.82	6.82	-171.16	1.7197	6.5105	61.07	61
26	59	60	86.82	86.82	-26.497	0.0768	0.0429	20.19	20.52
27	60	61	1.399	1.399	-84.558	0.1719	-0.0054	18.81	18.59
28	61	62	19.52	19.52	-31.818	0.0458	-0.8087	8.24	8.21
29	63	62	-55.992	-55.992	-73.576	0.0983	0.0492	20.33	19.56
30	56	64	86.229	86.229	45.201	0.2628	0.2043	21.17	20.02
31*	64	63	5.331	4.701	-9.486	0.0019	-0.5308	2.3	3.01
32	65	63	111.801	111.741	116.518	1.234	3.4051	34.38	34.92
33	21	24	149.868	149.868	29.221	0.1862	-1.7124	23.73	24.26
34	24	23	149.681	149.681	30.934	0.6244	-5.4993	23.81	24.33
35*	67	68	-6.801	-6.504	29.955	0.5661	0.1798	48.98	59.07
36	68	59	-6.198	-6.198	30.038	0.3066	0.0826	59.43	58.11
37	66	61	-83.29	-83.208	-92.794	1.8138	3.5814	27.5	27.18
38	22	23	-25.89	-25.87	22.854	0.0401	-13.5986	3.69	4.18
39	23	25	126.605	126.605	36.985	1.2857	-15.3612	20.73	20.81
40	71	69	-9.547	-9.547	-29.733	2.3647	0.447	51.78	57.97
41	70	71	-56.986	-56.986	-44.285	0.0675	-0.2584	14.69	14.69
42	71	72	27.859	27.859	12.825	0.0376	-1.4277	6.24	6.24
43	71	73	6.128	6.128	-4.585	0.0755	-1.8158	13.57	13.49
44	27	22	-18.189	-18.189	-60.976	0.1499	-56.6225	6.82	1.96
45	28	27	-25.327	-25.327	-29.888	0.0538	-42.1683	4.13	3.06
46	25	26	43.536	43.536	-9.155	0.0896	-13.3176	7.18	7.17
47	73	74	-10.886	-10.886	-4.058	0.0691	-2.3184	11.98	11.31
48	29	26	-27.67	-27.67	-47.164	0.1523	-20.5685	8.84	6.06
49	73	77	2.814	2.814	11.74	0.1525	-1.0058	21.46	21.68
50	78	77	-4.935	-4.932	8.709	0.2002	-1.7415	18.1	21.44
51	76	78	18.456	18.456	43.496	0.6212	0.4179	84.71	84.98
52	76	75	-0.339	-0.336	-1.476	0.0004	-3.2639	2.71	3.26
53	78	79	14.999	14.999	8.157	0.6175	-1.3946	31.22	31.22
54	73	80	6.682	6.682	3.283	0.1254	-2.2472	13.24	13.28
55	30	29	-63.079	-63.079	-80.011	0.3911	-11.1001	16.2	14.57
56	31	30	-105.46	-105.46	-14.153	1.6022	-39.8091	16.61	16.99
57	31	32	32.602	32.602	-55.979	0.1799	-55.3246	6.8	6.81
58	30	33	29.964	29.964	-60.342	0.1741	-34.5958	7.15	7.13
59	28	36	44.809	44.809	-56.02	0.243	-43.4286	7.53	7.54
60	35	34	39.828	39.828	-12.14	0.2742	-23.9784	8.7	8.7
61	34	37	19.796	19.796	-19.94	0.0639	-17.3922	5.91	5.92

74 47 15 205.879 205.879 136.795 1.2204 -5.9977 26.02 75 17 16 -46.401 -46.401 -104.05 0.3114 -13.591 12.13 76 43 48 0.001 0.001 -11.073 0.0006 -11.0732 1.17 77 18 19 215.64 215.64 -28.964 1.9432 -15.8997 22.84										
64 39 40 3.364 3.364 -13.247 0.0044 -15.7502 2.87 65* 36 35 43.621 43.558 -18.151 0.1018 -31.0326 3.9 66 32 28 -31.895 -31.895 -41.716 0.1246 -64.7544 5.51 67 33 41 28.244 28.244 -26.704 0.0587 -39.3359 4.09 68 42 46 16.729 16.729 -43.671 0.0609 -37.0599 4.95 69 43 42 42.126 42.126 7.731 0.109 -27.0672 4.51 70 41 43 42.81 5.955 0.0108 -3.2179 4.55 71 46 45 0.002 0.002 -17.29 0.0023 -17.2895 1.82 72 42 44 12.034 12.034 -11.037 0.0051 -19.0579 1.73 73 14 4	62	37 3	38	13.483	13.483	-6.487	0.0166	-13.046	3.14	3.14
65* 36 35 43.621 43.558 -18.151 0.1018 -31.0326 3.9 66 32 28 -31.895 -31.895 -41.716 0.1246 -64.7544 5.51 67 33 41 28.244 28.244 -26.704 0.0587 -39.3359 4.09 68 42 46 16.729 16.729 -43.671 0.0609 -37.0599 4.95 69 43 42 42.126 42.126 7.731 0.109 -27.0672 4.51 70 41 43 42.81 5.955 0.0108 -3.2179 4.55 71 46 45 0.002 0.002 -17.29 0.0023 -17.2895 1.82 72 42 44 12.034 12.034 -11.037 0.0051 -19.0579 1.73 73 14 47 206.258 206.258 134.747 0.3796 -2.0487 25.81 74 47 <	63	38 3	39	10.106	10.106	-17.205	0.0216	-23.5717	4.19	4.2
66 32 28 -31.895 -31.895 -41.716 0.1246 -64.7544 5.51 67 33 41 28.244 28.244 -26.704 0.0587 -39.3359 4.09 68 42 46 16.729 16.729 -43.671 0.0609 -37.0599 4.95 69 43 42 42.126 7.731 0.109 -27.0672 4.51 70 41 43 42.81 5.955 0.0108 -3.2179 4.55 71 46 45 0.002 0.002 -17.29 0.0023 -17.2895 1.82 72 42 44 12.034 12.034 -11.037 0.0051 -19.0579 1.73 73 14 47 206.258 206.258 134.747 0.3796 -2.0487 25.81 74 47 15 205.879 205.879 136.795 1.2204 -5.9977 26.02 75 17 16 <td< td=""><td>64</td><td>39 4</td><td>40</td><td>3.364</td><td>3.364</td><td>-13.247</td><td>0.0044</td><td>-15.7502</td><td>2.87</td><td>2.87</td></td<>	64	39 4	40	3.364	3.364	-13.247	0.0044	-15.7502	2.87	2.87
67 33 41 28.244 28.244 -26.704 0.0587 -39.3359 4.09 68 42 46 16.729 16.729 -43.671 0.0609 -37.0599 4.95 69 43 42 42.126 42.126 7.731 0.109 -27.0672 4.51 70 41 43 42.81 5.955 0.0108 -3.2179 4.55 71 46 45 0.002 0.002 -17.29 0.0023 -17.2895 1.82 72 42 44 12.034 12.034 -11.037 0.0051 -19.0579 1.73 73 14 47 206.258 206.258 134.747 0.3796 -2.0487 25.81 74 47 15 205.879 205.879 136.795 1.2204 -5.9977 26.02 75 17 16 -46.401 -46.401 -104.05 0.3114 -13.591 12.13 76 43	65*	36 3	35	43.621	43.558	-18.151	0.1018	-31.0326	3.9	4.92
68 42 46 16.729 16.729 -43.671 0.0609 -37.0599 4.95 69 43 42 42.126 42.126 7.731 0.109 -27.0672 4.51 70 41 43 42.81 42.81 5.955 0.0108 -3.2179 4.55 71 46 45 0.002 0.002 -17.29 0.0023 -17.2895 1.82 72 42 44 12.034 12.034 -11.037 0.0051 -19.0579 1.73 73 14 47 206.258 206.258 134.747 0.3796 -2.0487 25.81 74 47 15 205.879 205.879 136.795 1.2204 -5.9977 26.02 75 17 16 -46.401 -46.401 -104.05 0.3114 -13.591 12.13 76 43 48 0.001 0.001 -11.073 0.0006 -11.0732 1.17 77	66	32 2	28	-31.895	-31.895	-41.716	0.1246	-64.7544	5.51	4.12
69 43 42 42.126 42.126 7.731 0.109 -27.0672 4.51 70 41 43 42.81 42.81 5.955 0.0108 -3.2179 4.55 71 46 45 0.002 0.002 -17.29 0.0023 -17.2895 1.82 72 42 44 12.034 12.034 -11.037 0.0051 -19.0579 1.73 73 14 47 206.258 206.258 134.747 0.3796 -2.0487 25.81 74 47 15 205.879 205.879 136.795 1.2204 -5.9977 26.02 75 17 16 -46.401 -46.401 -104.05 0.3114 -13.591 12.13 76 43 48 0.001 0.001 -11.073 0.0006 -11.0732 1.17 77 18 19 215.64 215.64 -28.964 1.9432 -15.8997 22.84	67	33 4	41	28.244	28.244	-26.704	0.0587	-39.3359	4.09	4.07
70 41 43 42.81 42.81 5.955 0.0108 -3.2179 4.55 71 46 45 0.002 0.002 -17.29 0.0023 -17.2895 1.82 72 42 44 12.034 12.034 -11.037 0.0051 -19.0579 1.73 73 14 47 206.258 206.258 134.747 0.3796 -2.0487 25.81 74 47 15 205.879 205.879 136.795 1.2204 -5.9977 26.02 75 17 16 -46.401 -46.401 -104.05 0.3114 -13.591 12.13 76 43 48 0.001 0.001 -11.073 0.0006 -11.0732 1.17 77 18 19 215.64 215.64 -28.964 1.9432 -15.8997 22.84	68	42 4	46	16.729	16.729	-43.671	0.0609	-37.0599	4.95	4.95
71 46 45 0.002 0.002 -17.29 0.0023 -17.2895 1.82 72 42 44 12.034 12.034 -11.037 0.0051 -19.0579 1.73 73 14 47 206.258 206.258 134.747 0.3796 -2.0487 25.81 74 47 15 205.879 205.879 136.795 1.2204 -5.9977 26.02 75 17 16 -46.401 -46.401 -104.05 0.3114 -13.591 12.13 76 43 48 0.001 0.001 -11.073 0.0006 -11.0732 1.17 77 18 19 215.64 215.64 -28.964 1.9432 -15.8997 22.84	69	43 4	42	42.126	42.126	7.731	0.109	-27.0672	4.51	4.51
72 42 44 12.034 -11.037 0.0051 -19.0579 1.73 73 14 47 206.258 206.258 134.747 0.3796 -2.0487 25.81 74 47 15 205.879 205.879 136.795 1.2204 -5.9977 26.02 75 17 16 -46.401 -46.401 -104.05 0.3114 -13.591 12.13 76 43 48 0.001 0.001 -11.073 0.0006 -11.0732 1.17 77 18 19 215.64 215.64 -28.964 1.9432 -15.8997 22.84	70	41 4	43	42.81	42.81	5.955	0.0108	-3.2179	4.55	4.55
73 14 47 206.258 206.258 134.747 0.3796 -2.0487 25.81 74 47 15 205.879 205.879 136.795 1.2204 -5.9977 26.02 75 17 16 -46.401 -46.401 -104.05 0.3114 -13.591 12.13 76 43 48 0.001 0.001 -11.073 0.0006 -11.0732 1.17 77 18 19 215.64 215.64 -28.964 1.9432 -15.8997 22.84	71	46 4	45	0.002	0.002	-17.29	0.0023	-17.2895	1.82	1.82
74 47 15 205.879 205.879 136.795 1.2204 -5.9977 26.02 75 17 16 -46.401 -46.401 -104.05 0.3114 -13.591 12.13 76 43 48 0.001 0.001 -11.073 0.0006 -11.0732 1.17 77 18 19 215.64 215.64 -28.964 1.9432 -15.8997 22.84	72	42 4	44	12.034	12.034	-11.037	0.0051	-19.0579	1.73	1.73
75 17 16 -46.401 -46.401 -104.05 0.3114 -13.591 12.13 76 43 48 0.001 0.001 -11.073 0.0006 -11.0732 1.17 77 18 19 215.64 215.64 -28.964 1.9432 -15.8997 22.84	73	14 4	47	206.258	206.258	134.747	0.3796	-2.0487	25.81	26.28
76 43 48 0.001 0.001 -11.073 0.0006 -11.0732 1.17 77 18 19 215.64 215.64 -28.964 1.9432 -15.8997 22.84	74	47 1	15	205.879	205.879	136.795	1.2204	-5.9977	26.02	26.5
77 18 19 215.64 215.64 -28.964 1.9432 -15.8997 22.84	75	17 1	16	-46.401	-46.401	-104.05	0.3114	-13.591	12.13	10.09
	76	43 4	48	0.001	0.001	-11.073	0.0006	-11.0732	1.17	1.17
78 19 21 346.746 346.746 -52.698 1.2023 -0.6658 37.02	77	18 1	19	215.64	215.64	-28.964	1.9432	-15.8997	22.84	23.34
	78	19 2	21	346.746	346.746	-52.698	1.2023	-0.6658	37.02	37.81
79 49 41 -37.802 -37.802 -31.954 0.1982 -76.1153 5.21	79	49 4	41	-37.802	-37.802	-31.954	0.1982	-76.1153	5.21	6.13
80 81 80 4.563 4.563 -4.2 0.0984 -5.2088 8.66	80	81 8	80	4.563	4.563	-4.2	0.0984	-5.2088	8.66	8.67
81 15 22 -92.743 -92.743 -13.178 0.1749 -9.916 10.04	81	15 2	22	-92.743	-92.743	-13.178	0.1749	-9.916	10.04	9.73
total 46.7367 -1917.23	total						46.7367	-1917.23		

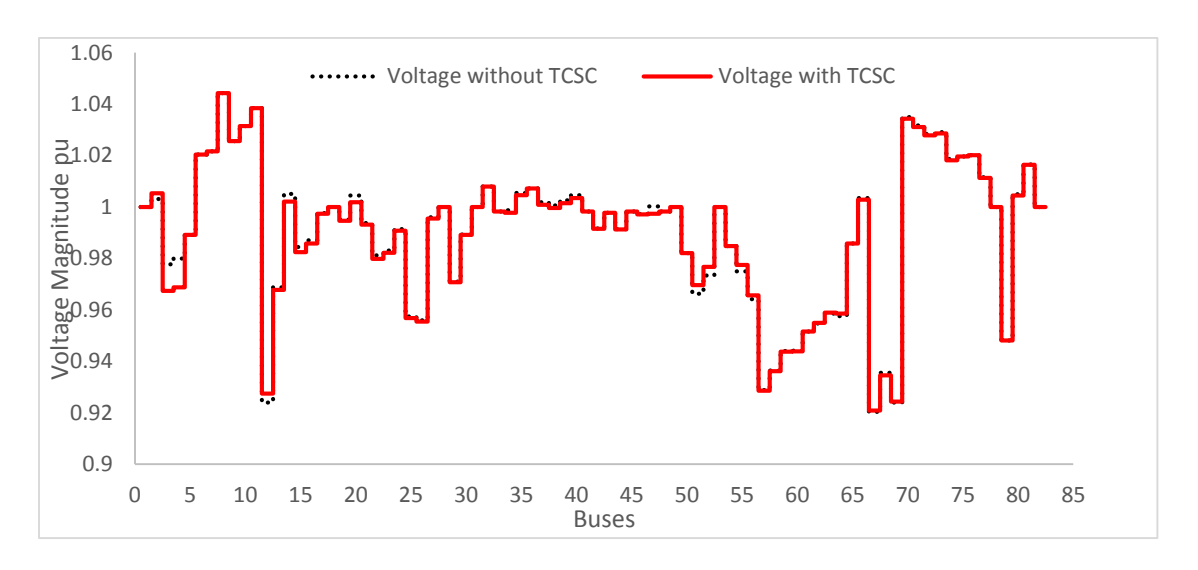


Figure 4.12: Voltage Magnitude with and without TCSC.

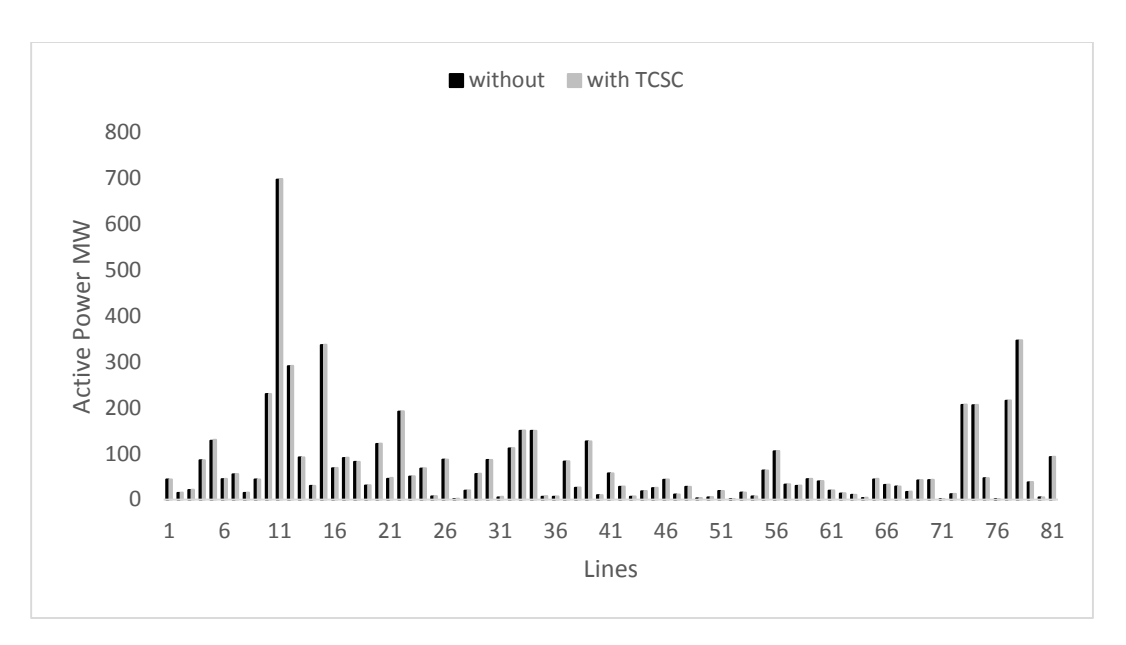


Figure 4.13: Active power with and without TCSC.

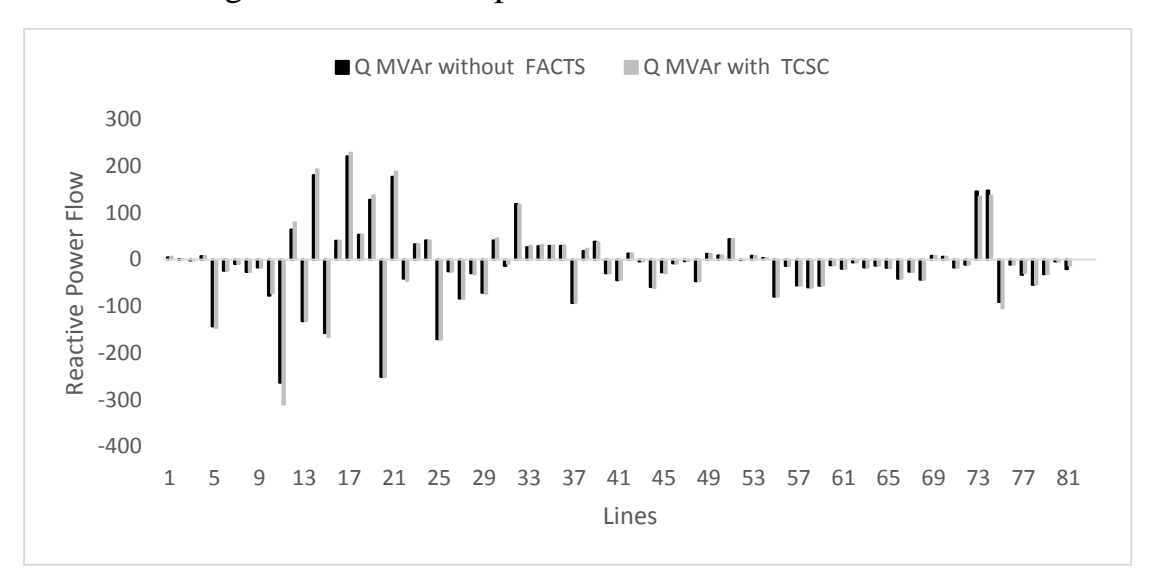


Figure 4.14: Reactive power with and without TCSC.

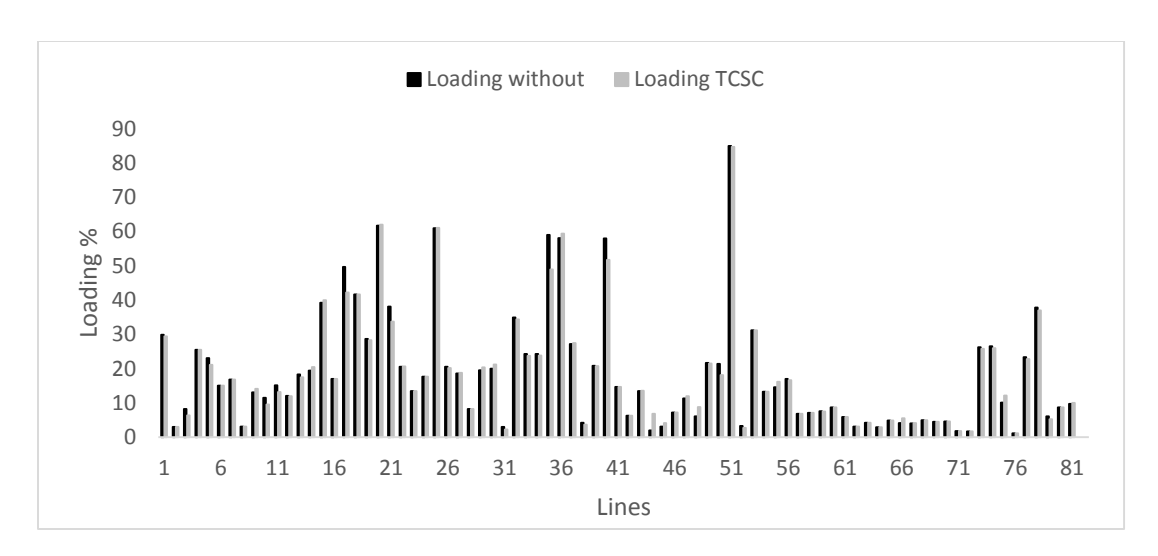


Figure 4.15: Transmission lines loading with and without TCSC.

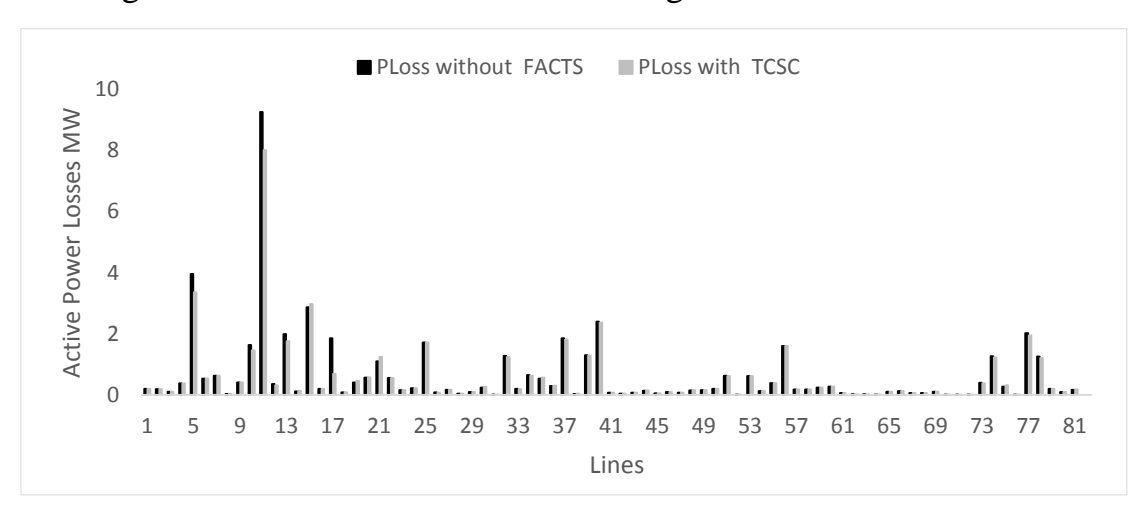


Figure 4.16: Active power Losses with and without TCSC.

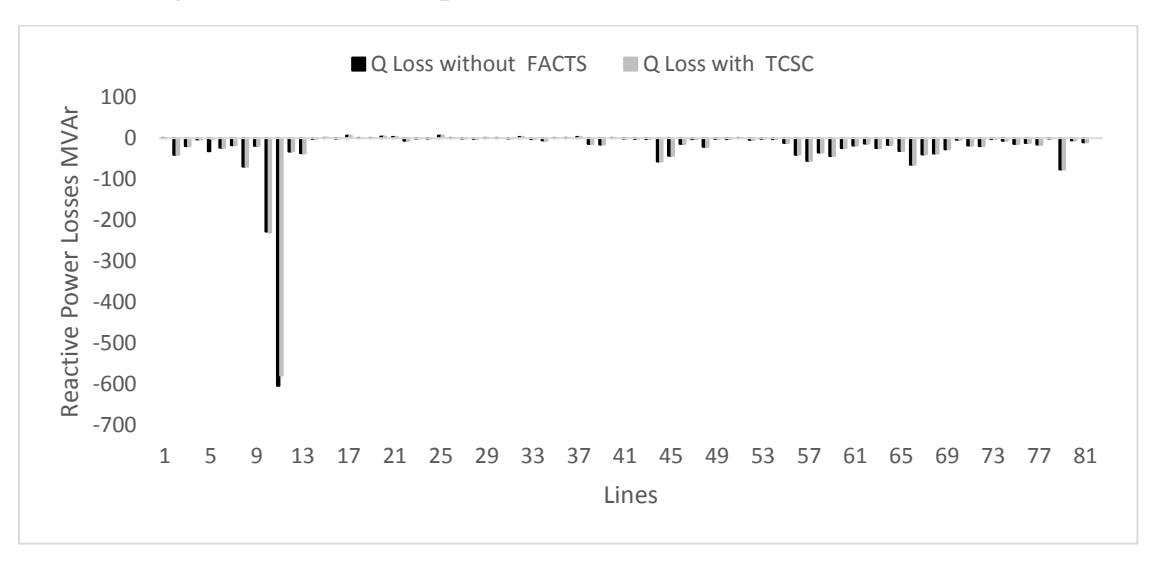
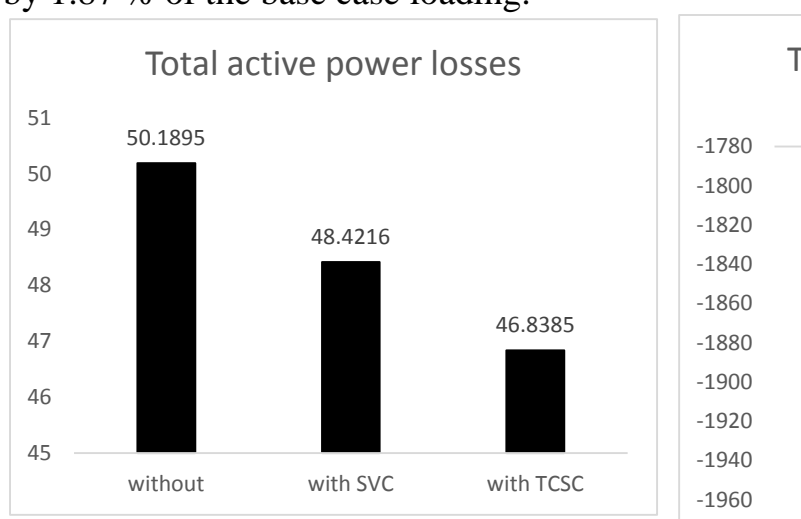


Figure 4.17: Reactive power Losses with and without TCSC.

From Figure 4.12 to Figure 4.17, As expected, The voltage profile after incorporation TCSC do not changes compared with the base case, It should be noticed that the effect of TCSC is clear in the active power losses more than voltage magnitude, as in Figure 4.11 and Figure 4.15, any TCSC connected with line the power losses decrease due to the line impedance decrease by X_{TCSC} also the active and reactive power flow increased in these line. Loading of lines decreased only in the line connected with TCSC. The overall loading of the system has been decreased by 1.87 % of the base case loading.



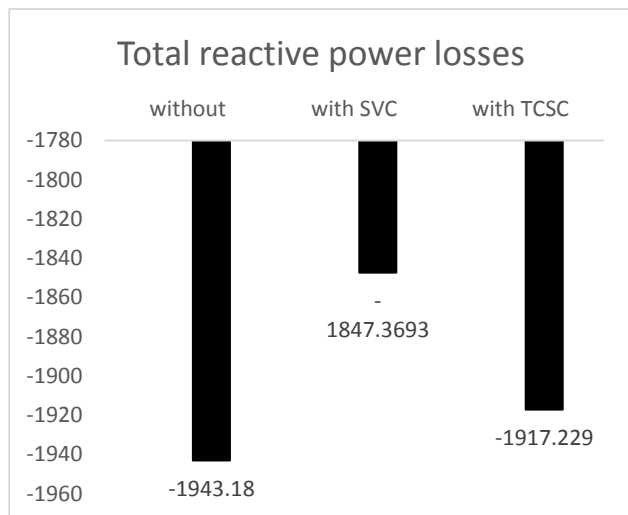
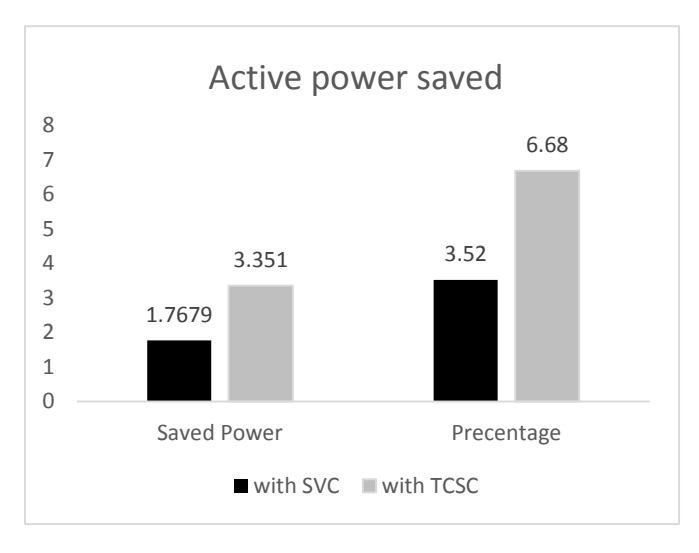


Figure 4.18: Total active & reactive power Losses without and with FACTS



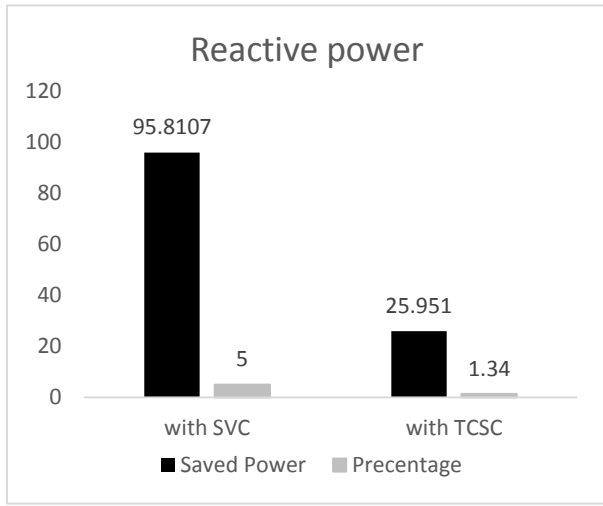


Figure 4.19 Total saved power and percentage improvement.

It can be observed from Figure 4.18 the total real power losses decrease when implement SVC and TCSC to the Sudanese grid. Active power losses when installing SVC greater than active power losses when installing TCSC. Figures 4.19 shows the overall power losses improvement and the energy saved by installing the FACTS controllers.

As a result of installing Four SVC controller in the Sudanese national grid, the voltage of the network have been improved, and the reactive power losses have been reduced, also it can be Observed that the SVC controller does not have a direct effect on the active power flow and active power losses. The propose installing strategy have been introduced for TCSC controller, seven TCSC controller have been install in the system and result on reducing the active power losses and increasing the power transfer capability. From obtained results it can be observed the TCSC controller have a poor effect on the voltage magnitude of the buses and the reactive power losses.

CHAPTER FIVE

CONCLUSION AND RECOMMENDATIONS

5.1 CONCLUSION

Recently power losses and voltage instability problems are the major problems in power system and generation cost also goes higher. FACTS concept made a revolution in power system which overcomes all the problems. Many techniques are used to optimize the location of FACTS controllers. The stability indices is used as an optimization technique in this dissertation. The results show that voltage profile is enhanced at all buses and power losses are considerably decreased by considering the objectives such as minimization of voltage stability index, minimization of power losses and minimization of generation cost and also there is a reduction in power loss when compared with the base case.

Both SVC and TCSC capable of increasing static voltage stability margin, though SVC provides higher voltage stability margin and better voltage profiles compared to TCSC because the SVC is a shunt compensation device, which inject the reactive power at the connected bus (weakest bus) where power system requires reactive power the most at this bus. Injection of reactive power at this bus using SVC can improve voltage stability margin farther. However the TCSC is series compensation devices, which inject reactive power through the connected line. This may not be effective when the system required reactive power at the load bus.

5.2 RECOMMENDATIONS

In this dissertation, the impact of SVC and TCSC on Sudanese National Grid is investigated. Following issues needs more investigation:

- Implement of other FACTS controllers such as STATCOM, SSSC, UPFC and IPFC to improve performance and prevent sudden instability.
- Implementation multi-type of FACTS controllers.
- Implementation a new optimization methods to select the optimal placement of FACTS controllers such as Genetics Algorithm GA, Particle Swarm Optimization PSO and other Artificial Intelligence.
- Control schemes and intelligent controllers can be considered for FACTS controllers.
- Investigation economic balance to conclude whether it is economically viable to invest on FACTS, i.e. to calculate the money losses due to the under exploitation of the transmission lines and the saved and invested money on FACTS.

REFERENCES

- [1] D.K. Sharma, Aziz Ahmad, Richa Saluja, Reena Parmar," *Voltage Stability in Power system Using STATCOM*', IJECSE, ISSN-2277-1956
- [2] Enrique Acha, C. R. Fuerte, Hugo A. Pe'rez, C. A. Camacho, "FACTS Modelling and Simulation in Power Networks", John Wiley & Sons Ltd, West Sussex PO19 8SQ, England, ISBN 0-470-85271-2, Copyright © 2004
- [3] K. R. Padiyar," Facts Controllers In Power Transmission And Distribution", New Age International Publishers, 2007.
- [4] Christine E. Doig Cardet, "Analysis on Voltage Stability Indices", Institute for Automation of Complex Power Systems, Germany.
- [5] K.R. Padiyar, " *Power System Dynamics Stability and Control*", Second Edition, BS Publications, Hyderabad, 2002.
- [6] P. R. Sharma & Anirudh Dube "Location of SVC and UPFC for Real Power Loss Minimization and Stability Enhancement in a Multi Machine Power System using Parametric Approach", IJAEEE, Volume-1, Issue-1, 2012.
- [7] Omorogiuwa Eseosa1, Friday Osasere Odiase "Efficiency Improvement of Nigeria 330kv Network Using Flexible Alternating Current Transmission System (Facts) Devices" International Journal of Advances in Engineering & Technology, VOL.4 Issue 1, pp 26-41, July 2012.
- [8] Chakraborty A, Haldar S, "Power System Analysis Operation and Control". Prentice-Hall, 2008 India
- [9] Shraddha Udgir, Sarika Varshney & Laxmi Srivastava," *Optimal Placement and Sizing of SVC For Improving Voltage Profile of Power System*", International

- Journal of Power System Operation and Energy Management, Volume-1, Issue-2, 2011.
- [10] Hassan M.O, S. J. Cheng, Z. A. Zakaria "Steady-State Modeling of SVC And TCSC For Power Flow Analysis". IMECS, Hong Kong, 18–20 Mar 2009.
- [11]Ali Abdulwahhab Abdulrazzaq, "Improving The Power System Performance Using FACTS Devices", IOSR-JEEE, Volume 10, Issue 2 Ver. IV(Mar Apr. 2015), PP 41-49.
- [12]S. B. Bhaladhare, P.P. Bedekar," *Enhancement of Voltage Stability Through Optimal Location Of SVC*", IJECSE, Volume 2.
- [13] Kiran Kumar Kuthadi, N. Suresh J.E, "Enhancement of Voltage Stability Through Optimal Placement of Facts Controllers In Power Systems", vol 1, Issue 1, July 2012.
- [14] Sarita Bhole, Prateek Nigam," *Improvement of Voltage Stability In Power System By Using SVC And Statcom*", IJISET, Vol. 2 Issue 4, April 2015.
- [15] Nemat-Talebi, M. Ehsan, "An Efficient Power Injection Modeling and Sequential Power Flow Algorithm For FACTS Devices", Southeast Con, Proceedings. IEEE pp-97-104, ISBN: 0-7803-8368-0, March 2004.
- [16]T.Pavan Kumar, A.Lakshmi Devi, "Optimal Location and Parameter Settings Of TCSC Under Single Line Contingency Using PSO Technique", IJAERS, Vol. I, Issue I/October-December, 2011/30-34.
- [17]M.Senthil Kumar, P.Renuga," *Bacterial Foraging Algorithm Based Enhancement of Voltage Profile and Minimization of Losses Using Thyristor Controlled Series Capacitor (TCSC)*", International Journal of Computer Applications (0975 8887) Volume 7– No.2, September 2010.

- [18] A. R. Phadke, S. K. Bansal ,K. R. Niazi," *A Comparison of Voltage Stability Indices For Placing Shunt FACTS Controllers*", ICETET.2008.30.
- [19] N.A.M.Ismail, A.A.M.Zin, A.Khairuddin, S.Khokhar," *A Comparison of Voltage Stability Indices*", 2014 IEEE 8th International Power Engineering and Optimization Conference (PEOCO2014), Langkawi, The Jewel of Kedah, Malaysia. 24-25 March 2014.
- [20] Ismail Musirin., Titik Khawa Abdul Rahman," *On-Line Voltage Stability Based Contingency Ranking Using Fast Voltage Stability Index (FVSI)*", IEEE, 2002.
- [21] NEPLAN Software tutorial.

APPENDICES

Appendix A: Sudanese electrical network data.

• Bus data:

Bus number	Type*	Pg MW	Qg MVAr	Pd MW	Qd MVAr	Bs MVAr	Base KV
1	3	0	0	0	0	-125	500
2	1	0	0	0	0	-125	500
3	1	0	0	0	0	-250	500
4	1	0	0	0	0	0	500
5	1	0	0	14.36	11.483	-30	220
6	1	0	0	0	0	-40	220
7	1	0	0	33.456	23.961	0	220
8	1	0	0	0	0	0	220
9	1	0	0	50.32	46.148	0	220
10	1	0	0	29.808	20.496	0	220
11	1	0	0	0	0	0	220
12	1	0	0	101.338	70.734	0	220
13	1	0	0	33.264	20.615	0	220
14	1	0	0	0	0	0	220
15	1	0	0	0	0	0	220
16	1	0	0	0	0	0	220
17	1	0	0	13.574	8.661	0	220
18	2	186	0	0	0	0	220
19	1	0	0	0	0	0	220
20	1	0	0	60.883	37.732	0	220
21	1	0	0	0	0	0	220
22	1	0	0	0	0	0	220
23	1	0	0	14.112	8.746	0	220
24	1	0	0	0	0	0	220
25	1	0	0	0	0	0	220
26	1	0	0	0	0	0	220
27	1	0	0	6.989	25.534	0	220
28	2	85	0	46.704	32.357	0	220
29	1	0	0	16.464	8.842	0	220
30	1	0	0	12.029	5.585	0	220
31	2	148	0	8.333	5.76	-15	220
32	1	0	0	0.403	22.385	0	220
33	1	0	0	1.546	0.958	0	220
34	1	0	0	19.757	31.778	0	220
35	1	0	0	3.629	25.117	0	220
36	1	0	0	1.008	5.56	0	220
37	1	0	0	6.25	3.939	0	220
38	1	0	0	3.36	23.764	0	220
39	1	0	0	6.72	4.568	-15	220
40	1	0	0	3.36	2.503	0	220
41	1	0	0	0	0	-30	220
42	1	0	0	0	0	0	220
43	1	0	0	0.672	12.515	0	220

44	1	0	0	12.029	8.021	0	220
45	1	0	0	0	0	0	220
46	1	0	0	16.666	10.678	0	220
47	1	0	0	0	0	0	220
48	1	0	0	0	0	0	220
49	2	38	0	0	0	-30	220
50	1	0	0	81.917	53.127	0	110
51	1	0	0	68.006	39.992	0	110
52	1	0	0	41.328	17.854	0	110
53	2	76	0	0	0	0	110
54	1	0	0	44.621	20.718	0	110
55	1	0	0	74.189	46.562	0	110
56	1	0	0	12.634	8.128	15	110
57	1	0	0	50.266	33.255	0	110
58	1	0	0	17.203	8.477	0	110
59	1	0	0	40.387	18.165	0	110
60	1	0	0	85.344	58.018	0	110
61	1	0	0	64.915	40.06	0	110
62	1	0	0	75.466	42.566	0	110
63	1	0	0	59.069	30.588	0	110
64	1	0	0	81.312	54.43	0	110
65	1	0	0	0	0	0	110
66	1	0	0	0	0	0	110
67	1	0	0	36.49	24.236	0	110
68	1	0	0	0	0	0	110
69	1	0	0	0	0	0	110
70	1	0	0	24.73	12.738	0	110
71	1	0	0	11.088	5.864	0	110
72	1	0	0	27.821	14.253	0	110
73	1	0	0	56.717	26.986	0	110
74	1	0	0	10.886	4.058	0	110
75	1	0	0	0.336	1.476	0	110
76	1	0	0	0	0	0	110
77	1	0	0	7.594	4.037	0	110
78	2	7	0	4.704	2.238	0	110
79	1	0	0	14.381	9.552	0	110
80	1	0	0	11.021	6.539	0	110
81	1	0	0	18.614	12.315	0	110
82	2	2	0	15.254	8.604	0	66

 $^{*1 =} PQ, \overline{2 = PV, 3 = Slack}$

• Line data at MVAbase = 1000.

	From	To	R	X	В	rating	ratio
	bus	bus	p.u.	p.u.	p.u.	MVA	
_	67	69	0.086281	0.10438	9.81E-05	93.5	1
	6	5	0.283781	1.279132	4.07E-02	213.84	1
	11	10	0.054252	0.287679	4.74E-03	187	1
	9	7	0.218861	1.16054	1.91E-02	187	1
	12	13	0.096901	0.436777	5.56E-02	213.84	1

10	7	0.218421	1.158209	1.91E-02	187	1
11	8	0.272988	1.447553	2.38E-02	187	1
9	6	0.114897	0.461302	6.59E-02	275	1
9	8	0.218861	1.16054	1.91E-02	187	1
2	1	0.02651	0.261317	2.43E-01	1064	1
1	3	0.019376	0.190992	7.11E-01	1064	1
4	3	0.004122	0.040627	3.78E-02	1064	1
13	17	0.079597	0.319576	4.57E-02	275	1
18	17	0.003461	0.013895	1.99E-03	275	1
16	19	0.020764	0.093595	1.19E-02	213.84	1
52	51	0.030455	0.122273	1.09E-03	137.5	1
54	50	0.00886	0.03557	3.18E-04	137.5	1
53	52	0.033223	0.133388	1.19E-03	137.5	1
55	56	0.022149	0.088926	7.94E-04	137.5	1
54	53	0.00714	0.056157	3.25E-04	132	1
53	55	0.033223	0.133388	1.19E-03	137.5	1
14	20	0.014535	0.058357	8.34E-03	275	1
59 5 9	58	0.030455	0.122273	1.09E-03	137.5	1
58	57	0.03876	0.15562	1.39E-03	137.5	1
59	54	0.052488	0.228653	1.05E-03	85.8	1
59	60	0.008306	0.033347	2.98E-04	137.5	1
60	61	0.021595	0.086702	7.74E-04	137.5	1
61	62	0.030455	0.122273	1.09E-03	137.5	1
62	63	0.010521	0.04224	3.77E-04	137.5	1
64	63	0.016335	0.065583	5.86E-04	137.5	1
56	64	0.025748	0.10376	9.23E-04	137.5	1
65	63	0.045682	0.183409	1.64E-03	137.5	1
21	24	0.007851	0.041632	2.74E-03	187	1
24	23	0.025909	0.137386	9.05E-03	187	1
68	67	0.517686	0.626281	5.88E-04	31.57	1
59	68	0.287603	0.347934	3.27E-04	31.57	1
61	66 22	0.107975	0.433512 0.100041	3.87E-03	137.5	1 1
23 23	25	0.024917 0.067521	0.100041	1.43E-02 2.36E-02	275 187	1
23 69	23 71	2.214545	2.679091	2.50E-02 2.52E-03	31.57	1
71	71	0.013843	0.055579	2.32E-03 4.96E-04	137.5	1
71	70 72	0.013643	0.033379	4.90E-04 1.49E-03	137.5	1
71	73	1.581818	1.913636	1.49E-03 1.80E-03	31.57	1
22	27	0.10223	0.410447	5.87E-02	275	1
27	28	0.10223	0.297901	4.26E-02	275	1
25	26	0.043182	0.228977	1.51E-02	187	1
74	73	0.566653	1.559645	2.40E-03	55	1
26	29	0.06595	0.349711	2.40E-03 2.30E-02	187	1
73	77	1.006612	1.217769	1.14E-03	31.57	1
77	78	1.72562	2.087603	1.96E-03	31.57	1
76	78	0.287603	0.347934	3.27E-04	31.57	1
75	76 76	2.760992	3.340165	3.14E-03	31.57	1
78	79	1.984463	2.400744	2.26E-03	31.57	1
73	80	2.041983	2.470331	2.32E-03	31.57	1
29	30	0.039256	0.208161	1.37E-02	187	1
30	31	0.139752	0.741054	4.88E-02	187	1
			•			_

31 32 0.096901 0.38905 5.56E-02 275 1 30 33 0.062293 0.250103 3.57E-02 275 1 28 36 0.076829 0.308461 4.41E-02 275 1 35 34 0.174421 0.700289 2.50E-02 275 1 34 37 0.123202 0.494649 1.77E-02 275 1 37 38 0.091364 0.366818 1.31E-02 275 1 38 39 0.164731 0.661384 2.36E-02 275 1 39 40 0.10936 0.43907 1.57E-02 275 1 36 35 0.054195 0.21759 3.11E-02 275 1 28 32 0.11282 0.452965 6.47E-02 275 1 42 46 0.065754 0.263998 3.77E-02 275 1 41 43 0.005707 0.022912							
28 36 0.076829 0.308461 4.41E-02 275 1 35 34 0.174421 0.700289 2.50E-02 275 1 34 37 0.123202 0.494649 1.77E-02 275 1 37 38 0.091364 0.366818 1.31E-02 275 1 38 39 0.164731 0.661384 2.36E-02 275 1 39 40 0.10936 0.43907 1.57E-02 275 1 36 35 0.054195 0.21759 3.11E-02 275 1 28 32 0.11282 0.452965 6.47E-02 275 1 42 46 0.065754 0.263998 3.77E-02 275 1 42 44 0.033825 0.135806 1.94E-02 275 1 43 42 0.04845 0.194525 2.78E-02 275 1 44 43 0.030288 0.121606	31	32	0.096901	0.38905	5.56E-02	275	1
35 34 0.174421 0.700289 2.50E-02 275 1 34 37 0.123202 0.494649 1.77E-02 275 1 37 38 0.091364 0.366818 1.31E-02 275 1 38 39 0.164731 0.661384 2.36E-02 275 1 39 40 0.10936 0.43907 1.57E-02 275 1 36 35 0.054195 0.21759 3.11E-02 275 1 28 32 0.11282 0.452965 6.47E-02 275 1 42 46 0.065754 0.263998 3.77E-02 275 1 41 43 0.005707 0.022912 3.27E-03 275 1 41 43 0.005707 0.022912 3.27E-03 275 1 41 43 0.005707 0.022912 3.27E-03 275 1 42 44 0.033825 0.135806	30	33	0.062293	0.250103	3.57E-02	275	1
34 37 0.123202 0.494649 1.77E-02 275 1 37 38 0.091364 0.366818 1.31E-02 275 1 38 39 0.164731 0.661384 2.36E-02 275 1 39 40 0.10936 0.43907 1.57E-02 275 1 36 35 0.054195 0.21759 3.11E-02 275 1 36 35 0.054195 0.21759 3.11E-02 275 1 38 32 0.11282 0.452965 6.47E-02 275 1 42 46 0.065754 0.263998 3.77E-02 275 1 41 43 0.005707 0.022912 3.27E-03 275 1 41 43 0.005707 0.022912 3.27E-03 275 1 41 43 0.005707 0.022912 3.27E-02 275 1 42 44 0.033825 0.135806	28	36	0.076829	0.308461	4.41E-02	275	1
37 38 0.091364 0.366818 1.31E-02 275 1 38 39 0.164731 0.661384 2.36E-02 275 1 39 40 0.10936 0.43907 1.57E-02 275 1 36 35 0.054195 0.21759 3.11E-02 275 1 28 32 0.11282 0.452965 6.47E-02 275 1 33 41 0.069215 0.277893 3.97E-02 275 1 42 46 0.065754 0.263998 3.77E-02 275 1 41 43 0.005707 0.022912 3.27E-03 275 1 43 42 0.04845 0.194525 2.78E-02 275 1 44 4.0333825 0.135806 1.94E-02 275 1 44 4.03030288 0.121606 1.74E-02 275 1 47 15 0.01938 0.07781 1.11E-02 27	35	34	0.174421	0.700289	2.50E-02	275	1
38 39 0.164731 0.661384 2.36E-02 275 1 39 40 0.10936 0.43907 1.57E-02 275 1 36 35 0.054195 0.21759 3.11E-02 275 1 28 32 0.11282 0.452965 6.47E-02 275 1 33 41 0.069215 0.277893 3.97E-02 275 1 42 46 0.065754 0.263998 3.77E-02 275 1 41 43 0.005707 0.022912 3.27E-03 275 1 43 42 0.04845 0.194525 2.78E-02 275 1 43 42 0.04845 0.194525 2.78E-02 275 1 44 4.033825 0.135806 1.94E-02 275 1 46 45 0.030288 0.121606 1.74E-02 275 1 47 15 0.01938 0.07781 1.11E-02 <td>34</td> <td>37</td> <td>0.123202</td> <td>0.494649</td> <td>1.77E-02</td> <td>275</td> <td>1</td>	34	37	0.123202	0.494649	1.77E-02	275	1
39 40 0.10936 0.43907 1.57E-02 275 1 36 35 0.054195 0.21759 3.11E-02 275 1 28 32 0.11282 0.452965 6.47E-02 275 1 33 41 0.069215 0.277893 3.97E-02 275 1 42 46 0.065754 0.263998 3.77E-02 275 1 41 43 0.005707 0.022912 3.27E-03 275 1 43 42 0.04845 0.194525 2.78E-02 275 1 42 44 0.033825 0.135806 1.94E-02 275 1 46 45 0.030288 0.121606 1.74E-02 275 1 44 47 0.006229 0.02501 3.57E-03 275 1 47 15 0.01938 0.07781 1.11E-02 275 1 43 48 0.01938 0.07781	37	38	0.091364	0.366818	1.31E-02	275	1
36 35 0.054195 0.21759 3.11E-02 275 1 28 32 0.11282 0.452965 6.47E-02 275 1 33 41 0.069215 0.277893 3.97E-02 275 1 42 46 0.065754 0.263998 3.77E-02 275 1 41 43 0.005707 0.022912 3.27E-03 275 1 43 42 0.04845 0.194525 2.78E-02 275 1 42 44 0.033825 0.135806 1.94E-02 275 1 46 45 0.030288 0.121606 1.74E-02 275 1 46 45 0.030288 0.121606 1.74E-02 275 1 47 15 0.01938 0.07781 1.11E-02 275 1 47 15 0.01938 0.07781 1.11E-02 275 1 43 48 0.01938 0.07781	38	39	0.164731	0.661384	2.36E-02	275	1
28 32 0.11282 0.452965 6.47E-02 275 1 33 41 0.069215 0.277893 3.97E-02 275 1 42 46 0.065754 0.263998 3.77E-02 275 1 41 43 0.005707 0.022912 3.27E-03 275 1 43 42 0.04845 0.194525 2.78E-02 275 1 42 44 0.033825 0.135806 1.94E-02 275 1 46 45 0.030288 0.121606 1.74E-02 275 1 46 45 0.030288 0.121606 1.74E-02 275 1 47 15 0.01938 0.07781 1.11E-02 275 1 47 15 0.01938 0.07781 1.11E-02 275 1 43 48 0.01938 0.07781 1.11E-02 275 1 18 19 0.041529 0.166736	39	40	0.10936	0.43907	1.57E-02	275	1
33 41 0.069215 0.277893 3.97E-02 275 1 42 46 0.065754 0.263998 3.77E-02 275 1 41 43 0.005707 0.022912 3.27E-03 275 1 43 42 0.04845 0.194525 2.78E-02 275 1 42 44 0.033825 0.135806 1.94E-02 275 1 46 45 0.030288 0.121606 1.74E-02 275 1 46 45 0.030288 0.121606 1.74E-02 275 1 47 15 0.01938 0.07781 1.11E-02 275 1 47 15 0.01938 0.07781 1.11E-02 275 1 43 48 0.01938 0.07781 1.11E-02 275 1 48 19 0.041529 0.166736 2.38E-02 275 1 49 21 0.00969 0.38905	36	35	0.054195	0.21759	3.11E-02	275	1
42 46 0.065754 0.263998 3.77E-02 275 1 41 43 0.005707 0.022912 3.27E-03 275 1 43 42 0.04845 0.194525 2.78E-02 275 1 42 44 0.033825 0.135806 1.94E-02 275 1 46 45 0.030288 0.121606 1.74E-02 275 1 46 45 0.030288 0.121606 1.74E-02 275 1 47 15 0.01938 0.07781 1.11E-02 275 1 47 15 0.01938 0.07781 1.11E-02 275 1 43 48 0.01938 0.07781 1.11E-02 275 1 43 48 0.01938 0.07781 1.11E-02 275 1 18 19 0.041529 0.166736 2.38E-02 275 1 41 49 0.134277 0.539112	28	32	0.11282	0.452965	6.47E-02	275	1
41 43 0.005707 0.022912 3.27E-03 275 1 43 42 0.04845 0.194525 2.78E-02 275 1 42 44 0.033825 0.135806 1.94E-02 275 1 46 45 0.030288 0.121606 1.74E-02 275 1 14 47 0.006229 0.02501 3.57E-03 275 1 47 15 0.01938 0.07781 1.11E-02 275 1 16 17 0.026302 0.105599 1.51E-02 275 1 43 48 0.01938 0.07781 1.11E-02 275 1 43 48 0.01938 0.07781 1.11E-02 275 1 18 19 0.041529 0.166736 2.38E-02 275 1 41 49 0.134277 0.539112 7.71E-02 275 1 81 80 4.400331 5.019917	33	41	0.069215	0.277893	3.97E-02	275	1
43 42 0.04845 0.194525 2.78E-02 275 1 42 44 0.033825 0.135806 1.94E-02 275 1 46 45 0.030288 0.121606 1.74E-02 275 1 14 47 0.006229 0.02501 3.57E-03 275 1 47 15 0.01938 0.07781 1.11E-02 275 1 16 17 0.026302 0.105599 1.51E-02 275 1 43 48 0.01938 0.07781 1.11E-02 275 1 43 48 0.01938 0.07781 1.11E-02 275 1 18 19 0.041529 0.166736 2.38E-02 275 1 19 21 0.00969 0.038905 5.56E-03 275 1 41 49 0.134277 0.539112 7.71E-02 275 1 81 80 4.400331 5.019917	42	46	0.065754	0.263998	3.77E-02	275	1
42 44 0.033825 0.135806 1.94E-02 275 1 46 45 0.030288 0.121606 1.74E-02 275 1 14 47 0.006229 0.02501 3.57E-03 275 1 47 15 0.01938 0.07781 1.11E-02 275 1 16 17 0.026302 0.105599 1.51E-02 275 1 43 48 0.01938 0.07781 1.11E-02 275 1 18 19 0.041529 0.166736 2.38E-02 275 1 18 19 0.041529 0.166736 2.38E-02 275 1 19 21 0.00969 0.038905 5.56E-03 275 1 41 49 0.134277 0.539112 7.71E-02 275 1 81 80 4.400331 5.019917 5.21E-03 40.7 1 22 15 0.01938 0.087355	41	43	0.005707	0.022912	3.27E-03	275	1
46 45 0.030288 0.121606 1.74E-02 275 1 14 47 0.006229 0.02501 3.57E-03 275 1 47 15 0.01938 0.07781 1.11E-02 275 1 16 17 0.026302 0.105599 1.51E-02 275 1 43 48 0.01938 0.07781 1.11E-02 275 1 43 48 0.01938 0.07781 1.11E-02 275 1 18 19 0.041529 0.166736 2.38E-02 275 1 18 19 0.041529 0.166736 2.38E-02 275 1 19 21 0.00969 0.038905 5.56E-03 275 1 41 49 0.134277 0.539112 7.71E-02 275 1 81 80 4.400331 5.019917 5.21E-03 40.7 1 22 15 0.01938 0.087355	43	42	0.04845	0.194525	2.78E-02	275	1
14 47 0.006229 0.02501 3.57E-03 275 1 47 15 0.01938 0.07781 1.11E-02 275 1 16 17 0.026302 0.105599 1.51E-02 275 1 43 48 0.01938 0.07781 1.11E-02 275 1 18 19 0.041529 0.166736 2.38E-02 275 1 18 19 0.041529 0.166736 2.38E-02 275 1 19 21 0.00969 0.038905 5.56E-03 275 1 41 49 0.134277 0.539112 7.71E-02 275 1 81 80 4.400331 5.019917 5.21E-03 40.7 1 22 15 0.01938 0.087355 1.11E-02 213.84 1 25 70 0 0.51333 0 300 0.905 59 21 0 0.596 0	42	44	0.033825	0.135806	1.94E-02	275	1
47 15 0.01938 0.07781 1.11E-02 275 1 16 17 0.026302 0.105599 1.51E-02 275 1 43 48 0.01938 0.07781 1.11E-02 275 1 18 19 0.041529 0.166736 2.38E-02 275 1 19 21 0.00969 0.038905 5.56E-03 275 1 41 49 0.134277 0.539112 7.71E-02 275 1 81 80 4.400331 5.019917 5.21E-03 40.7 1 22 15 0.01938 0.087355 1.11E-02 213.84 1 25 70 0 0.511333 0 300 0.905 59 21 0 0.596 0 300 0.922 52 19 0 0.643333 0 450 0.905 12 2 0 0.393333 0 600	46	45	0.030288	0.121606	1.74E-02	275	1
16 17 0.026302 0.105599 1.51E-02 275 1 43 48 0.01938 0.07781 1.11E-02 275 1 18 19 0.041529 0.166736 2.38E-02 275 1 19 21 0.00969 0.038905 5.56E-03 275 1 41 49 0.134277 0.539112 7.71E-02 275 1 81 80 4.400331 5.019917 5.21E-03 40.7 1 22 15 0.01938 0.087355 1.11E-02 213.84 1 25 70 0 0.511333 0 300 0.905 59 21 0 0.596 0 300 0.922 52 19 0 0.643333 0 450 0.905 12 2 0 0.393333 0 600 0.905 16 4 0 0.56 0 900	14	47	0.006229	0.02501	3.57E-03	275	1
43 48 0.01938 0.07781 1.11E-02 275 1 18 19 0.041529 0.166736 2.38E-02 275 1 19 21 0.00969 0.038905 5.56E-03 275 1 41 49 0.134277 0.539112 7.71E-02 275 1 81 80 4.400331 5.019917 5.21E-03 40.7 1 22 15 0.01938 0.087355 1.11E-02 213.84 1 25 70 0 0.511333 0 300 0.905 59 21 0 0.596 0 300 0.922 52 19 0 0.643333 0 450 0.905 12 2 0 0.393333 0 600 0.905 16 4 0 0.56 0 900 0.915 3 14 0 0.56 0 900 0.975	47	15	0.01938	0.07781	1.11E-02	275	1
18 19 0.041529 0.166736 2.38E-02 275 1 19 21 0.00969 0.038905 5.56E-03 275 1 41 49 0.134277 0.539112 7.71E-02 275 1 81 80 4.400331 5.019917 5.21E-03 40.7 1 22 15 0.01938 0.087355 1.11E-02 213.84 1 25 70 0 0.511333 0 300 0.905 59 21 0 0.596 0 300 0.922 52 19 0 0.643333 0 450 0.905 12 2 0 0.393333 0 600 0.905 16 4 0 0.56 0 600 0.915 3 14 0 0.56 0 900 0.911 41 81 0 1.2 0 200 0.905 <tr< td=""><td>16</td><td>17</td><td>0.026302</td><td>0.105599</td><td>1.51E-02</td><td>275</td><td>1</td></tr<>	16	17	0.026302	0.105599	1.51E-02	275	1
19 21 0.00969 0.038905 5.56E-03 275 1 41 49 0.134277 0.539112 7.71E-02 275 1 81 80 4.400331 5.019917 5.21E-03 40.7 1 22 15 0.01938 0.087355 1.11E-02 213.84 1 25 70 0 0.511333 0 300 0.905 59 21 0 0.596 0 300 0.922 52 19 0 0.643333 0 450 0.905 12 2 0 0.393333 0 600 0.905 16 4 0 0.56 0 600 0.915 3 14 0 0.56 0 900 0.911 41 81 0 1.2 0 200 0.975 42 82 0 1.253 0 200 0.918 <td< td=""><td>43</td><td>48</td><td>0.01938</td><td>0.07781</td><td>1.11E-02</td><td>275</td><td>1</td></td<>	43	48	0.01938	0.07781	1.11E-02	275	1
41 49 0.134277 0.539112 7.71E-02 275 1 81 80 4.400331 5.019917 5.21E-03 40.7 1 22 15 0.01938 0.087355 1.11E-02 213.84 1 25 70 0 0.511333 0 300 0.905 59 21 0 0.596 0 300 0.922 52 19 0 0.643333 0 450 0.905 12 2 0 0.3933333 0 600 0.905 16 4 0 0.56 0 600 0.915 3 14 0 0.56 0 900 0.911 41 81 0 1.2 0 200 0.975 42 82 0 1.253 0 200 0.905 26 73 0 0.7045 0 200 0.918 69 23 0 1.34 0 150 0.905 29 76	18	19	0.041529	0.166736	2.38E-02	275	1
81 80 4.400331 5.019917 5.21E-03 40.7 1 22 15 0.01938 0.087355 1.11E-02 213.84 1 25 70 0 0.511333 0 300 0.905 59 21 0 0.596 0 300 0.922 52 19 0 0.643333 0 450 0.905 12 2 0 0.393333 0 600 0.905 16 4 0 0.56 0 600 0.915 3 14 0 0.56 0 900 0.911 41 81 0 1.2 0 200 0.975 42 82 0 1.253 0 200 0.905 26 73 0 0.7045 0 200 0.918 69 23 0 1.34 0 150 0.905 29 76 0 1.424545 0 110 0.945 56 20	19	21	0.00969	0.038905	5.56E-03	275	1
22 15 0.01938 0.087355 1.11E-02 213.84 1 25 70 0 0.511333 0 300 0.905 59 21 0 0.596 0 300 0.922 52 19 0 0.643333 0 450 0.905 12 2 0 0.393333 0 600 0.905 16 4 0 0.56 0 600 0.915 3 14 0 0.56 0 900 0.911 41 81 0 1.2 0 200 0.975 42 82 0 1.253 0 200 0.905 26 73 0 0.7045 0 200 0.918 69 23 0 1.34 0 150 0.905 29 76 0 1.424545 0 110 0.945 56 20	41	49	0.134277	0.539112	7.71E-02	275	1
25 70 0 0.511333 0 300 0.905 59 21 0 0.596 0 300 0.922 52 19 0 0.643333 0 450 0.905 12 2 0 0.393333 0 600 0.905 16 4 0 0.56 0 600 0.915 3 14 0 0.56 0 900 0.911 41 81 0 1.2 0 200 0.975 42 82 0 1.253 0 200 0.905 26 73 0 0.7045 0 200 0.918 69 23 0 1.34 0 150 0.905 29 76 0 1.424545 0 110 0.945 56 20 0 0.844667 0 450 0.975 15 65 0 0.858 0 300 0.925 1 11 0 0.243	81	80	4.400331	5.019917	5.21E-03	40.7	1
59 21 0 0.596 0 300 0.922 52 19 0 0.643333 0 450 0.905 12 2 0 0.393333 0 600 0.905 16 4 0 0.56 0 600 0.915 3 14 0 0.56 0 900 0.911 41 81 0 1.2 0 200 0.975 42 82 0 1.253 0 200 0.905 26 73 0 0.7045 0 200 0.918 69 23 0 1.34 0 150 0.905 29 76 0 1.424545 0 110 0.945 56 20 0 0.844667 0 450 0.975 15 65 0 0.858 0 300 0.925 1 11 0	22	15	0.01938	0.087355	1.11E-02	213.84	1
52 19 0 0.643333 0 450 0.905 12 2 0 0.393333 0 600 0.905 16 4 0 0.56 0 600 0.915 3 14 0 0.56 0 900 0.911 41 81 0 1.2 0 200 0.975 42 82 0 1.253 0 200 0.905 26 73 0 0.7045 0 200 0.918 69 23 0 1.34 0 150 0.905 29 76 0 1.424545 0 110 0.945 56 20 0 0.844667 0 450 0.975 15 65 0 0.858 0 300 0.925 1 11 0 0.243778 0 900 0.967	25	70	0	0.511333	0	300	0.905
12 2 0 0.393333 0 600 0.905 16 4 0 0.56 0 600 0.915 3 14 0 0.56 0 900 0.911 41 81 0 1.2 0 200 0.975 42 82 0 1.253 0 200 0.905 26 73 0 0.7045 0 200 0.918 69 23 0 1.34 0 150 0.905 29 76 0 1.424545 0 110 0.945 56 20 0 0.844667 0 450 0.975 15 65 0 0.858 0 300 0.925 1 11 0 0.243778 0 900 0.967	59	21	0	0.596	0	300	0.922
16 4 0 0.56 0 600 0.915 3 14 0 0.56 0 900 0.911 41 81 0 1.2 0 200 0.975 42 82 0 1.253 0 200 0.905 26 73 0 0.7045 0 200 0.918 69 23 0 1.34 0 150 0.905 29 76 0 1.424545 0 110 0.945 56 20 0 0.844667 0 450 0.975 15 65 0 0.858 0 300 0.925 1 11 0 0.243778 0 900 0.967	52	19	0	0.643333	0	450	0.905
3 14 0 0.56 0 900 0.911 41 81 0 1.2 0 200 0.975 42 82 0 1.253 0 200 0.905 26 73 0 0.7045 0 200 0.918 69 23 0 1.34 0 150 0.905 29 76 0 1.424545 0 110 0.945 56 20 0 0.844667 0 450 0.975 15 65 0 0.858 0 300 0.925 1 11 0 0.243778 0 900 0.967	12	2	0	0.393333	0	600	0.905
41 81 0 1.2 0 200 0.975 42 82 0 1.253 0 200 0.905 26 73 0 0.7045 0 200 0.918 69 23 0 1.34 0 150 0.905 29 76 0 1.424545 0 110 0.945 56 20 0 0.844667 0 450 0.975 15 65 0 0.858 0 300 0.925 1 11 0 0.243778 0 900 0.967	16	4	0	0.56	0	600	0.915
42 82 0 1.253 0 200 0.905 26 73 0 0.7045 0 200 0.918 69 23 0 1.34 0 150 0.905 29 76 0 1.424545 0 110 0.945 56 20 0 0.844667 0 450 0.975 15 65 0 0.858 0 300 0.925 1 11 0 0.243778 0 900 0.967	3	14	0	0.56	0	900	0.911
26 73 0 0.7045 0 200 0.918 69 23 0 1.34 0 150 0.905 29 76 0 1.424545 0 110 0.945 56 20 0 0.844667 0 450 0.975 15 65 0 0.858 0 300 0.925 1 11 0 0.243778 0 900 0.967	41	81	0	1.2	0	200	0.975
69 23 0 1.34 0 150 0.905 29 76 0 1.424545 0 110 0.945 56 20 0 0.844667 0 450 0.975 15 65 0 0.858 0 300 0.925 1 11 0 0.243778 0 900 0.967	42	82	0	1.253	0	200	0.905
29 76 0 1.424545 0 110 0.945 56 20 0 0.844667 0 450 0.975 15 65 0 0.858 0 300 0.925 1 11 0 0.243778 0 900 0.967	26	73	0	0.7045	0	200	0.918
56 20 0 0.844667 0 450 0.975 15 65 0 0.858 0 300 0.925 1 11 0 0.243778 0 900 0.967	69	23	0	1.34	0	150	0.905
15 65 0 0.858 0 300 0.925 1 11 0 0.243778 0 900 0.967	29	76	0	1.424545	0	110	0.945
1 11 0 0.243778 0 900 0.967	56	20	0	0.844667	0	450	0.975
	15	65	0	0.858	0	300	0.925
22 66 0 0.866667 0 150 0.913	1	11	0	0.243778	0	900	0.967
	22	66	0	0.866667	0	150	0.913

• Actual line data

	From	То	Length	R(1)	X(1)	C(1)	Un
			km	Ohm/	Ohm/	uF/	kV
-	BAG1	GAD B2	3	0.348	0.421	0.0086	110
	WWA2	WHL2	205	0.067	0.302	0.0131	220
	DON2	DEB2-B1	139.38	0.076	0.403	0.009	220
	MWP2	MWT2	34.55	0.076	0.403	0.009	220

ATB2	SHN2	140	0.0335	0.151	0.0261	220
MWP2	DEB2-B2	173.85	0.076	0.403	0.009	220
MWT2	DEB2-B1	139.1	0.076	0.403	0.009	220
DON2	WWA2	166	0.0335	0.1345	0.0261	220
DON2	DEB2-B2	139.38	0.076	0.403	0.009	220
ATB5	MWP500	236.7	0.028	0.276	0.0131	500
MWP500	MRK5	346	0.014	0.138	0.0262	500
KAB5	MRK5	36.8	0.028	0.276	0.0131	500
SHN2	FRZ2	115	0.0335	0.1345	0.0261	220
GER2	FRZ2	5	0.0335	0.1345	0.0261	220
KAB2	IBA2	30	0.0335	0.151	0.0261	220
IBA1	IZB1	11	0.0335	0.1345	0.0261	110
KHN1	IBA1	12	0.0335	0.1345	0.0261	110
KUK1	KHE1	3.2	0.0335	0.1345	0.0261	110
IZG1	MHD1	8	0.0335	0.1345	0.0261	110
KUK1	KHN1	4.5	0.0192	0.151	0.019	110
KHN1	IZG1	12	0.0335	0.1345	0.0261	110
MRK2	MHD2	21	0.0335	0.1345	0.0261	220
AFR1	FAR1	14	0.0335	0.1345	0.0261	110
KLX1	AFR1	11	0.0335	0.1345	0.0261	110
KLX1	KUK1	14.6	0.0435	0.1895	0.019	110
KLX1	LOM1	3	0.0335	0.1345	0.0261	110
LOM1	SHG1	7.8	0.0335	0.1345	0.0261	110
SHG1	MUG`	11	0.0335	0.1345	0.0261	110
MUG`	BNT1	3.8	0.0335	0.1345	0.0261	110
MHD1	OMD1	9.3	0.0335	0.135	0.0261	110
OMD1	BNT1	5.9	0.0335	0.1345	0.0261	110
GAM1	BNT1	16.5	0.0335	0.1345	0.0261	110
KLX2	SOB2	10	0.038	0.2015	0.018	220
SOB2	GAD2	33	0.038	0.2015	0.018	220
SOB1 B2	BAG1	18	0.348	0.421	0.0086	110
KLX1	SOB1 B2	10	0.348	0.421	0.0086	110
SHG1	JAS1	39	0.0335	0.1345	0.0261	110
GAD2	JAS2	36	0.0335	0.1345	0.0261	220
GAD2	NHAS2	86	0.038	0.2015	0.018	220
GAD B2	OHAS1	77	0.348	0.421	0.0086	110
OHAS1	NHAS1	5	0.0335	0.1345	0.0261	110
OHAS1	GND1	15	0.0335	0.1345	0.0261	110
OHAS1	MAR1 B1	55	0.348	0.421	0.0086	110
JAS2	MSH2	147.7	0.0335	0.1345	0.0261	220
MSH2	RBK2	107.2	0.0335	0.1345	0.0261	220
NHAS2	2-Mar	55	0.038	0.2015	0.018	220
MAN1	MAR1 B1	65.3	0.105	0.289	0.0097	110

2-Mar	SNJ2	84	0.038	0.2015	0.018	220
MAR1 B1	HAG1	35	0.348	0.421	0.0086	110
HAG1	SNP1	60	0.348	0.421	0.0086	110
SNJ 1	SNP1	10	0.348	0.421	0.0086	110
ORBK1	SNJ 1	96	0.348	0.421	0.0086	110
SNP1	MIN1	69	0.348	0.421	0.0086	110
MAR1 B1	FAO1	71	0.348	0.421	0.0086	110
SNJ2	SNG2	50	0.038	0.2015	0.018	220
SNG2	ROS2	178	0.038	0.2015	0.018	220
ROS2	RNK2	140	0.0335	0.1345	0.0261	220
SNG2	HWT2	90	0.0335	0.1345	0.0261	220
RBK2	TND2	111	0.0335	0.1345	0.0261	220
UMR2	OBD2	126	0.067	0.269	0.0131	220
OBD2	DBT2	89	0.067	0.269	0.0131	220
DBT2	ZBD2	66	0.067	0.269	0.0131	220
ZBD2	FUL2	119	0.067	0.269	0.0131	220
FUL2	BBN2	79	0.067	0.269	0.0131	220
TND2	UMR2	78.3	0.0335	0.1345	0.0261	220
RBK2	RNK2	163	0.0335	0.1345	0.0261	220
HWT2	GDF2	100	0.0335	0.1345	0.0261	220
GRB2	KSL2	95	0.0335	0.1345	0.0261	220
SHK2	GRB2	70	0.0335	0.1345	0.0261	220
GDF2	SHK2	8.245	0.0335	0.1345	0.0261	220
KSL2	ARO2	43.76	0.0335	0.1345	0.0261	220
GRB2	NHLF2	48.87	0.0335	0.1345	0.0261	220
MRK2	HUD	9	0.0335	0.1345	0.0261	220
HUD	GAM2	28	0.0335	0.1345	0.0261	220
KAB2	FRZ2	38	0.0335	0.1345	0.0261	220
SHK2	UTP2	28	0.0335	0.1345	0.0261	220
GER2	IBA2	60	0.0335	0.1345	0.0261	220
IBA2	KLX2	14	0.0335	0.1345	0.0261	220
GDF2	SHD2	194	0.0335	0.1345	0.0261	220
GDF 1	FAO1	153	0.348	0.397	0.009	110
JAS2	GAM2	28	0.0335	0.151	0.0261	220

Appendix B: MATLAB program to carry out the line stability index using CPF function of MATPOWER.

```
clear
clc
define constants;
mpcb = loadcase(case82);
mpopt = mpoption('pf.alg','NR','pf.tol',10^-3,
'pf.nr.max it',50);
lampda=1.4;
%set up target case with
mpc = mpcb;
%increased generation
mpc.gen(:,[PG QG])=mpcb.gen(:,[PG QG])*lampda;
%increased load
mpc.bus(:,[PD QD])=mpcb.bus(:,[PD QD])*lampda;
index=[];LQP=[];NVSI=[];FVSI=[];
results=runpf(mpc,mpopt);
X =mpc.branch(:,BR X);
R =mpc.branch(:,BR R);
Theta = atan(X./R);
Fbus =results.branch(:,F BUS);
Tbus =results.branch(:,T BUS);
VM =results.bus(:,VM);
Vangle =results.bus(:, VA);
Qr=results.branch(:,QT);
Qs=results.branch(:,QF);
for i=1:96
Vs(i) = VM(Fbus(i));
    Ds(i) = Vangle(Fbus(i));
    Dr(i) = Vangle(Tbus(i));
     if Or(i)<0
        Vs(i) = VM(Tbus(i));
          Ps(i) = abs(results.branch(i, PF));
          Or(i) = abs(results.branch(i,QT));
          Pr(i) = abs(results.branch(i,PT));
          end
LQP=4.*(X./Vs.^2).*(0.001^2.*(X./Vs.^2).*Ps.^2+0.001.*Qr);
FVSI = (4.*(R.^2+X.^2).*0.001.*Qr)./(Vs.^2.*X);
NVSI = (2.*X.*sqrt((0.001.*Pr).^2 + (0.001.*Qr).^2))./(2.*X.*0.001.*
Qr-Vs.^2);
index=[Fbus Tbus LQP FVSI NVSI];
```